Cholecystokinin-A receptors regulate photic input pathways to the circadian clock

Takao Shimazoe,* Mitsutaka Morita,* Shinichiro Ogiwara,† Tomoyoshi Kojiya,† Junpei Goto,† Masaki Kamakura,‡ Takahiro Moriya,§ Kazuyuki Shinohara,§ Soichi Takiguchi,‖ Akira Kono,‖ Kyoko Miyasaka,¶ Akihiro Funakoshi,‖ and Masayuki Ikeda†,#,1

*Graduate School of Pharmaceutical Sciences, Kyushu University, Fukuoka, Japan; †Graduate School of Science and Engineering, University of Toyama, Toyama, Japan; ‡Biotechnology Research Center, Faculty of Engineering, Toyama Prefectural University, Toyama, Japan; §Department of Translational Medical Sciences, Course of Medical and Dental Sciences, Nagasaki University Graduate School of Biomedical Sciences, Nagasaki, Japan; ‖National Kyushu Cancer Center, Fukuoka, Japan; ¶Department of Translational Medical Sciences, Tokyo Metropolitan Institute of Gerontology, Tokyo, Japan; and #Advanced Institute for Biological Science, Waseda University, Tokyo, Japan

ABSTRACT **Daily behaviors are strongly dominated by internally generated circadian rhythms, but the underlying mechanisms remain unclear. In mammals, photoentrainment of behaviors to light-dark cycles involves signaling from both intrinsically photosensitive retinal ganglion cells and classic photoreceptor pathways to the suprachiasmatic nucleus (SCN). How classic photoreceptor pathways work with the photosensitive ganglion cells, however, is not fully understood. Although cholecystokinin (CCK) peptide has been shown to be present in a variety of vertebrate retinas, its function at a systems level is also unknown. In the present study we examined a possible role of CCK-A receptors in photoentrainment using CCK-A receptor knockout mice. The lacZ reporter gene within a gene-knockout cassette revealed precise localization of CCK-A receptors in the circadian clock system. We demonstrated that CCK-A receptors were located predominately on glycinergic amacrine cells but were rarely found on SCN neurons. Moreover, Ca^{2+} imaging analysis demonstrated that the CCK-A agonist, CCK-8 sulfate (CCK-8s), mobilized intracellular Ca^{2+} in amacrine cells but not glutamate-receptive SCN neurons. Furthermore, light pulse-induced *mPer1/mPer2* gene expression in SCN, behavioral phase shifts, and the pupillary reflex were significantly reduced in CCK-A receptor knockout mice. These data indicate a novel function of CCK-A receptors in the nonimage-forming photoreception presumably *via* amacrine cell-mediated signal transduction pathways.—Shimazoe, T., Morita, M., Ogiwara, S., Kojiya, T., Goto, J., Kamakura, M., Moriya, T., Shinohara, K., Takiguchi, S., Kono, A., Miyasaka, K., Funakoshi, A., Ikeda, M. Cholecystokinin-A receptors regulate photic input pathways to the circadian clock. *FASEB J.* 22, 1479–1490 (2008)**

Key Words: cholecystokinin-A receptor mutant mice · glycinergic amacrine cells · melanopsin retinal ganglion cells · suprachiasmatic nucleus neurons

DAILY BEHAVIORAL RHYTHMS are strictly controlled by the hypothalamic suprachiasmatic nucleus (SCN), the mammalian circadian pacemaker (1, 2). Although these rhythms persist under time cue-free conditions, they are usually synchronized to the environmental light-dark cycles, a process called photoentrainment. The classic photoreceptor cells, rods and cones, are not the only cells involved in this process, however, because photoentrainment still occurs in mutant (*rd1a/rd*) mice lacking all rods and cones (3). It has been shown that intrinsically photosensitive retinal ganglion cells, which contain the pigment melanopsin (4), respond directly to light and send monosynaptic projections to the SCN and the olivary pretectal nuclei, as part of nonimage-forming visual functions including photoentrainment and the pupillary light reflex (5, 6). Photoentrainment is still possible, however, in melanopsin-deficient ($Opn4^{-/-}$) mice and only becomes absent with the subtraction of both the photosensitivity of retinal ganglion cells and classic photoreceptors in double mutant melanopsin-deficient and retinal degeneration ($Opn4^{-/-}$; *rd/rd*) mice (7). These results suggest that classic photoreceptors and intrinsically photosensitive retinal ganglion cells represent compensatory photoreception mechanisms for circadian photoentrainment. In mice, intrinsically photosensitive retinal ganglion cell dendrites in the inner ON region of the inner plexiform layer receive both bipolar and amacrine cell terminals, whereas intrinsically photosensitive retinal ganglion cell dendrites stratifying in the outer OFF region of the inner plexiform layer receive only amacrine cell terminals (8). The circuitry between photoreceptor pathways, retinal ganglion cells, and amacrine cells underlying photoentrainment, however, is not fully understood.

In SCN neurons, some subcellular responses have been identified that may be involved in photoentrainment. After photic stimulation at night, retino-recipient SCN neurons respond to glutamate release from reti-

[1] Correspondence: Department of Biology, Faculty of Science, University of Toyama, Rm. B214, 3190 Gofuku, Toyama-city, Toyama 930-8555, Japan. E-mail: msikeda@sci.u-toyama.ac.jp

doi: 10.1096/fj.07-9372com

nohypothalamic tract terminals with an activation of *N*-methyl-D-aspartate glutamate receptors, an increase in cytosolic Ca^{2+} concentration, and immediate expression of clock genes, such as *mPer1* and *mPer2* (9–11). Several other signaling mechanisms also appear to be involved. For example, pituitary adenylate cyclase-activating polypeptide is released from retinohypothalamic tract terminals in addition to glutamate (12), and serotonin-1B receptors (13) and GABA-B receptors (14) on retinohypothalamic tract terminals may synergistically control neurotransmitter release on SCN pacemaker neurons. The interconnections of these elements remain unclear, however.

Cholecystokinin (CCK) is one of the most abundant neuropeptides in the central nervous system, but its function in many pathways has not been identified. CCK immunoreactive cell bodies and axons have been shown to be sparsely dispersed throughout the SCN of rats, mice, and hamsters (6, 15–17). In addition, CCK peptide has been shown to be present in a variety of vertebrate retinas (18–21). In rat retinas, it is located predominantly in amacrine cells (22) and may function for local signal transduction pathways, as expression of CCK-A and CCK-B receptor mRNAs has been reported for retinal homogenates (23). The function of CCK within this circadian clock circuitry has not been elucidated, but it is a reasonable hypothesis that CCK peptides have a role in the SCN clock work itself and/or photic input pathways to the SCN. Indeed, we have reported that photoentrainment of locomotor rhythms and immediate early gene (*c-fos*) expression in SCN neurons in response to light are significantly reduced in Otsuka Long Evans Tokushima Fatty (OLETF) rats, a strain of obese mutant rats, that lack CCK-A receptor genes (24–27). Although these data are highly suggestive, multiple other genes are also lacking in OLETF rats; thus, further experiments are needed to identify the specific gene responsible for the circadian photoentrainment (28, 29).

To examine the specific function of CCK-A receptors in the circadian clock system, in the present study we used mutant mice lacking CCK-A receptors ($CCKAR^{-/-}$) that carry the lacZ reporter gene within a gene-knockout cassette (30), which allowed precise study of the localization of CCK-A receptors. We also examined the function of these receptors at the gene expression, intracellular signaling, and behavioral levels. Based on these data, we propose that CCK-A receptors on a subpopulation of retinal amacrine cells may have an important role in nonimage-forming visual functions.

MATERIALS AND METHODS

Mice

Male $CCKAR^{-/-}$ mice and their wild-type control littermates were generated as described previously (30). In short, the targeting vector was designed to replace the *SalI-BglI* 1.9-kb genomic fragment of the mouse CCK-A receptor gene with a NLS-lacZ and pGK-neo cassette. The homologous recombination deleted the first 122 amino acids, including the first membrane-spanning region of the CCK-A receptor. J1 embryonic stem (ES) cells were electroporated with the targeting vector and selected with G418 on embryonic fibroblast feeder cells. After Southern blot analysis screening, the successful ES clones were microinjected into blastocysts of C57BL/6J females. Finally, two independent ES clones generated germline chimeras. The chimeras were bred with C57BL6J mice to generate $CCKAR^{+/-}$ mutant F1 mice. $CCKAR^{-/-}$ mice were finally generated by mating $CCKAR^{+/-}$ mice followed by sufficient backcross to C57BL/6J wild-type mice. The experiments below were approved by the Committee of Animal Care of Kyusyu University and University of Toyama.

Locomotor activity recording

Wild-type and $CCKAR^{-/-}$ mice were housed in temperature-controlled (23±2°C) rooms, with a 12:12-h light-dark cycle. Food and water were provided *ad libitum*. To observe locomotor activity rhythms, mice were transferred to transparent plastic cages (30×35×17 cm), and their locomotor activity was measured using an infrared area sensor (F5B; Omron, Kyoto, Japan) located 30 cm above the surface of the cage. Locomotor activity was continuously recorded in 6-min epochs *via* a 48-channel parallel interface installed in a personal computer. To observe the free-running locomotor activity rhythm in constant darkness, wild-type (n=8) and $CCKAR^{-/-}$ (n=8) mice were housed in constant darkness for 2–3 wk. The free-running period during the first 2 wk was calculated using a χ^2 periodogram. For animals housed in constant darkness, circadian time 12 was defined as the onset of locomotor activities. To evaluate the response to photic stimuli, mice were maintained in constant darkness for 9 days and then exposed to a full-spectrum light pulse (15 min at 10–500 lux) at circadian time 16. The activity-onset delays in free-running rhythms were calculated on the basis of the distance between the two regression lines drawn from daily onset of locomotor activity for 7 days before and after the light pulse.

Pupillometry

Consensual pupillary constriction was measured in response to an adirectional light stimulus. Light was exposed for 60 s by a flexible-arm 100-W halogen lamp house (LA100USW; Hayashi Watch-Works Co. LTD., Tokyo, Japan), by which intensity was adjusted (20 or 100 lux at the animal levels) or maximized (>1000 lux). UV wavelength (<400 nm) was eliminated by a UV cut-filter installed in the lamp house. Adult male wild-type mice (n=5) and $CCKAR^{-/-}$ mice (n=4) were dark adapted for 1–2 h and placed on a custom-built stereotactic apparatus, by which animal movement was restricted by a 27 mmϕ polyethylene tube. Pupillary constriction was monitored with an infrared video system (BBCAM130 Night Vision-II; Timely Computer, Inc., Tokyo, Japan), which is composed of a digital charge-coupled device (CCD) camera centering on eight coaxial infrared (>850 nm) light-emitting diode arrays. At the end of the experiment, 1% atropine sulfate (Wako Pure Chemicals, Tokyo, Japan) dissolved in saline was dropped on the eye to estimate maximal pupil dimensions. Pupil dimensions were measured from the video images using Video Studio version 6.0 software (Ulead System, Inc., Tokyo, Japan). All experiments were conducted during the light period of 12:12-hour light-dark cycles.

5-Bromo-4-chloro-3-indoyl-β-D-galactopyranoside (X-gal) staining

Adult wild-type and $CCKAR^{+/-}$ mice (6 wk old) were used for the X-gal staining experiments. These animals were deeply anesthetized with an intraperitoneal injection of sodium pentobarbital (50 mg/kg body weight) and transcardially perfused with PBS for 5 min and then with ice-cold 2% paraformaldehyde in 0.1 M phosphate buffer for 15 min. Eyes

and the whole brain were removed and further fixed in the same fixative (4°C, 2 h). Then the vitreous and connective tissues were carefully removed from the eye, and the cerebellum and olfactory bulb were cut off from the brain in ice-cold PBS. The eyecups and brain tissue were immersed in 20% sucrose PBS and stored overnight. Frozen sections of 20 μm thickness were cut using a cryostat microtome and mounted on glass slides. These samples were then stained for 3 h at 37°C with a β-galactosidase (β-gal) staining kit (K1465–01; Invitrogen, Carlsbad, CA, USA) according to the manufacturer's instruction. As a negative control, samples from wild-type mice were also stained, but no staining was observed with a 3-h reaction period. These samples were imaged using a color CCD camera (Ds-5mc; Nikon, Tokyo, Japan) mounted on an inverted microscope (Axiovert 135TV with a Plan-Neofluar ×10 objective; Carl Zeiss, Thornwood, NY, USA).

Immunohistochemistry

Retinal frozen sections prepared as above were also used for immunofluorescence double-labeling studies. After three PBS rinses, the fixed samples were incubated in 10% donkey serum (Jackson ImmunoResearch Laboratories, West Grove, PA, USA) dissolved in 0.01% Triton X-100 (Sigma-Aldrich Corp., St. Louis, MO, USA) in PBS for 2 h at room temperature (22–26°C). As a first step, samples were incubated with 1:2000 mouse anti-β-galactosidase (Sigma-Aldrich Corp.) dissolved in 10% donkey serum in PBS for 24 h at 4°C. After three 20-min PBS rinses, samples were incubated in 1:200 Cy3-conjugated donkey anti-mouse IgG (Jackson ImmunoResearch Laboratories). As an additional staining step, 1:50 goat anti-Chx10 (Santa Cruz Biotechnology, Santa Cruz, CA, USA), 1:2000 goat anti-glycine transporter 1 (Chemicon International Inc., Temecula, CA, USA), 1:1000 goat anti-calretinin (Chemicon International Inc.), or 1:1000 rabbit anti-calbindin D28k (Chemicon International Inc.) was used as a primary antibody, and 1:200 fluorescein isothiocyanate (FITC) -conjugated donkey anti-goat IgG (Jackson ImmunoResearch Laboratories) or 1:200 FITC-conjugated donkey anti-rabbit IgG (Jackson ImmunoResearch Laboratories) was used as a secondary antibody. Double-labeled samples were embedded with Vectashield containing 4,6-diamidino-2-phenylindole (DAPI) (Vector Laboratories, Burlingame, CA, USA). The fluorescent images were acquired using a confocal laser-scanning unit (LSM510; Carl Zeiss) mounted on an inverted microscope (Axiovert 200M with an oil immersion objective lens, Plan-Apochromat ×63/1.40; Carl Zeiss).

Organotypic cultures

Wild-type and CCKAR$^{-/-}$ mouse pups (2–3 days old) were used to make organotypic cultures of retina and SCN. For retinal cultures, eyeballs were removed from the body after deep pentobarbital anesthesia and immediately immersed in ice-cold PBS. Under a stereomicroscope, the sclera and cornea were carefully torn and peeled off using fine forceps, and the neural retina was isolated. After removal of pigment epithelium and lens, the neural retina was trimmed using microscissors and placed in a 0.40-μm filter cup (Millicell-CM; Millipore, Bedford, MA, USA) with the ganglion cell layer being on the surface. The neural retinas on filter cups were transferred to standard six-well culture plates and cultured with 1 ml of low-glucose Dulbecco's modified Eagle's medium supplemented with 1:50 B-27 (Invitrogen), 5 μM forskolin (Sigma-Aldrich Corp.), 20 ng/ml brain-derived neurotrophic factor (Invitrogen), and 50 μg/ml gentamicin (Invitrogen). The medium was changed every other day until recording (7–14 days in culture). This procedure enables the survival of the outer and inner nuclear layers and the ganglion cell layer in the *in vitro* slice cultures (31).

SCN cultures were prepared as described previously (32). Briefly, coronal hypothalamic slices containing the SCN were cut using a vibrating-blade microtome in artificial cerebrospinal fluid containing 138.6 mM NaCl, 3.35 mM KCl, 21 mM $NaHCO_3$, 0.6 mM NaH_2PO_4, 9.9 mM D-glucose, 0.5 mM $CaCl_2$, and 3 mM $MgCl_2$ and bubbled with 95% O_2 and 5% CO_2. These slices were trimmed to an ~4-mm square containing the ventral end of the hypothalamus centered on the third ventricle. The slices were placed in Millicell-CM filter cups and cultured with 1 ml of medium consisting of 50% Eagle's basal medium, 25% Earle's balanced salt solution, and 25% heat-inactivated horse serum, supplemented with glucose and Glutamax (Invitrogen). The slice containing the rostrocaudal center of the SCN was used for further experiments. The SCN and retinal cultures were maintained in a CO_2 incubator at 35.5 ± 0.5°C and 5% CO_2.

Ca^{2+} imaging in retinal cultures

The retinal cultures on a membrane filter were incubated for 30 min in culture medium containing 10 μM Fura-2 AM (Molecular Probes, Eugene, OR, USA) in a CO_2 incubator at 35.5 ± 0.5°C and 5% CO_2 and rinsed 3× with buffered salt solution (BSS) consisting of 128 mM NaCl, 5 mM KCl, 2.7 mM $CaCl_2$, 1.2 mM $MgCl_2$, 1 mM Na_2HPO_4, 10 mM glucose, and 10 mM HEPES/NaOH (pH 7.3). Then the retinal cultures were gently removed from membrane filters using a fine brush and transferred to a recording chamber on the microscope. Fluorescent images were obtained with an upright microscope (Axioskop FS; Carl Zeiss) with a water immersion objective (Achroplan ×40 NA0.75; Carl Zeiss). The wavelength of the excitation UV light (340 or 380 nm pulse; 100 ms) was switched using a filter wheel (Lambda 10-2; Sutter Instruments, Novato, CA, USA). The UV light was generated by a full-spectrum 175-W xenon bulb (Lambda LS; Sutter) conducted to the microscope through a liquid light guide and reflected using a dichroic mirror (FT 395 nm; Carl Zeiss). The pair of fluorescent images were processed using a band-pass filter (BP 485–515 nm; Carl Zeiss) and exposed to a multiple-format cooled CCD camera (CoolSnap-FS; Photometrics, Tokyo, Japan) at 6-s intervals. The filter wheel and the CCD camera were controlled using digital imaging software (MetaFluor version 6.0; Japan Molecular Devices, Tokyo, Japan). The background fluorescence was also subtracted using the software. During recording, slices were placed in a 0.5-ml bath chamber and perfused with BSS supplemented with tetrodotoxin (0.5 μM) at a flow rate of 2.5 ml/min. CCK-8 sulfate (CCK-8s), lorglumide, thapsigargin (all purchased from Sigma-Aldrich Corp.), Ca^{2+}-free BSS, and 60 mM potassium (high K^+) BSS were applied by switching the perfusate.

Ca^{2+} imaging in SCN cultures

Isolation of neuronal and glial images is difficult in SCN slices using conventional Fura-2 AM staining methods; therefore, neuron-specific Ca^{2+} imaging was performed using a yellow cameleon 2.1 sensor linked to a neuron-specific enolase promoter (32). The cameleon-expressing SCN slice was cut from a filter cup and transferred into the microscope chamber together with the membrane filter. The Ca^{2+} response was observed as above using an upright microscope with an ×40 water-immersion objective. The SCN neurons were exposed to 440 ± 5 nm light using a liquid light guide lamp house (Lambda LS) with a band-pass filter (440NBD10; Omega Optical Inc., Brattleboro, VT, USA). The resultant fluorescence image was separated using a dichroic mirror (455DRLP; Omega Optical Inc.) and fed into double-view

optics (A4313; Hamamatsu Corporation, Bridgewater, NJ, USA), in which one image was split into bilateral images *via* internal reflection mirrors and processed using two dichroic mirrors (515 DRLPXR; Omega Optical Inc.) and band-pass filters (480DF30 and 535DF25 filters). The lamp house, shutter, and CCD camera were controlled as above using digital imaging software.

Quantitative reverse transcriptase-polymerase chain reaction (PCR)

Total RNA was extracted from mouse tissue using RNAzolB reagent (Tel-Test Inc., Friendswood, TX, USA). Mice were deeply anesthetized with ether, and their brains were quickly removed. Coronal brain slices (1 mm) were prepared using a rodent brain matrix (RBM-2000C; ASI Instruments, Warren, MI, USA), and the SCN was punched out bilaterally from the brain slices. The cDNAs of *mPer1* (GenBank accession number AF022992; sense, 5′-CCAGGCCCGGAGAACCTTTTT-3′; antisense, 5′-CGAAGTTTGAGCTCCCGAAGTG-3′), *mPer2* (GenBank accession number AF035830; sense, 5′-ACACCACCCCTTACAAGCTTC-3′; antisense, 5′-CGCTGGATGATGTCTGGCTC-3′), CCK-A receptor (GenBank accession number AK004730; sense, 5′-ACAGGAGTGAGCCATTCACCAGC-3′; antisense, 5′-GATGTTGGTGACAGTCCGCATCG-3′), and mouse glyceraldehyde-3-phosphate dehydrogenase (GAPDH) (GenBank accession number M32599; sense, 5′-GGGAAGCTTGTCATCAA-3′; antisense, 5′-TGCTTCA-CCACCTTCTTG-3′) were amplified using a program temperature control system PC-700 (ASTEC, Fukuoka, Japan). The reaction solution consisted of 2.5 μl of 10× PCR buffer (Boehringer Mannheim, Mannheim, Germany), 2.5 μl of 2.5 mM dNTP, 1.25 μl of 10 μM sense, 1.25 μl of 10 μM antisense, 17.0 μl of distilled water, 0.25 μl of *Taq* polymerase (Boehringer Mannheim), and 0.2 μl of 20 μCi [^{32}P]dCTP (Amersham Pharmacia Biotech, Ltd., Little Chalfont, Buckinghamshire, UK). The PCR product was run on a 5% acrylamide gel. Images were visualized using an imaging plate (BAS-IP MS 2040; Fujifilm, Tokyo, Japan) and analyzed using Image Gauge (Fujifilm). The exponential phase of GAPDH amplification in all experimental conditions was located between cycles 22 and 24, and the exponential phase of *mPer1* and *mPer2* was located between cycles 29 and 31. The amplified efficiency of GAPDH and *mPer1* or *mPer2* was quantified at cycle 30. The ratio of the amplified target to the amplified internal control was compared.

In situ hybridization

Mice were deeply anesthetized with ether and intracardially perfused with chilled saline (25 ml) followed by 0.1 M phosphate buffer (pH=7.4) containing 4% paraformaldehyde (25 ml). Brains were removed, postfixed in 0.1 M phosphate buffer containing 4% paraformaldehyde for 24 h at 4°C, and transferred into 20% sucrose in 0.1 M phosphate buffer for 72 h at 4°C. Slices (40 μm thick) that included the SCN were cut using a cryostat and divided into three equal groups from rostral to caudal regions for the measurement of *mPer1* and *mPer2* mRNAs. The *mPer1* and *mPer2* cRNA probes were a gift from Dr. Hitoshi Okamura at Kobe University (nucleotide positions: *mPer1*, 538–1752; *mPer2*, 1–638) for use in these *in situ* hybridization studies. Slices were placed in 2× standard sodium citrate (SSC) and were treated with 1 μg/ml proteinase K in 10 mM Tris-HCl buffer (pH=7.5) containing 10 mM EDTA for 10 min at 37°C, followed by treatment with 0.25% acetic anhydride in 0.1 M triethanolamine and 0.9% NaCl for 10 min. The slices were then incubated in hybridization buffer [60% formamide, 10% dextran sulfate, 10 mM Tris-HCl (pH=7.4), 1 mM EDTA, 0.6 M NaCl, Denhardt's solution (0.02% Ficoll, 0.02% polyvinyl pyrrolidone, and 0.02% bovine serum albumin), 0.2 mg/ml tRNA, and 0.25% sodium dodecyl sulfate] containing ^{33}P-labeled cRNA probes for 16 h at 60°C. Radioisotope (α[α-^{33}P]UTP; PerkinElmer Life and Analytical Sciences, Boston, MA, USA) -labeled antisense cRNA probes were made from restriction enzyme-linearized cDNA templates. After high-stringency posthybridization washes with 2× SSC/50% formamide, slices were treated with RNaseA (10 μg/ml) for 30 min at 37°C. Images were prepared as autoradiograms using BioMax MR film (Eastman Kodak, Rochester, NY, USA). After conversion into optical density by ^{14}C-autoradiographic microscales (Amersham Biosciences Corp., Piscataway, NJ, USA), they were analyzed using an image analysis system (MCID; Imaging Research, St. Catharines, ON, Canada). Further, mounted slices after exposure to X-ray film were dipped into emulsion (NTB2, diluted 1:1 with distilled water; Eastman-Kodak), air-dried for 3 h, and stored in light-tight slide boxes at 4°C for 3 wk. The slides were developed with a D19 developer (Eastman Kodak), fixed with Fujifix (Fujifilm), and counterstained with cresyl violet (Sigma-Aldrich Corp.).

Statistical analysis

All data are presented as means with SE. Unless otherwise noted, one-way ANOVA followed by Duncan's multiple-range tests was used for the statistical comparisons across multiple means. Two-tailed Student's *t* test was used for the pairwise comparisons. A 95% confidence level was considered to indicate statistical significance. The irradiance dependency for the pupillary light reflex was analyzed using two-way ANOVA. The irradiance response curve for circadian phase shifts was analyzed using a four-parameter Hill function using SigmaPlot software (version 7.1; SPSS Inc., Chicago, IL, USA).

RESULTS

Robust expression of CCK-A receptors in glycinergic amacrine cells in the photic input pathways to the circadian clock

To visualize CCK-A receptors in the photic input pathways to the SCN clock, we examined X-gal staining using serial sections of retina and brain of heterozygous mutant (CCKAR$^{+/-}$) mice. In the retina, staining was robust throughout the inner nuclear layer (**Fig. 1*A***). Within the SCN, only scattered staining was observed in the core region, whereas the shell boundary zone (peri-SCN) and periventricular zone contained a relatively larger number of stained cells (Fig. 1*B*). The number of stained cells in the SCN was less than that in control hypothalamic regions, such as in the arcuate nuclei (number of X-gal stained cells=23.8±6.6/SCN slice and 137.6±19.4/rostral arcuate nucleus slice, number of slices=5, $P<0.01$ by Student's *t* test; Fig. 1*C*).

To determine the cell types in the retina that express CCK-A receptors, we examined double immunofluorescent staining of retina with antibodies against β-gal and several different neural markers (**Fig. 2**). Staining with the amacrine cell marker, glycine transporter-1, was strongly colocalized with β-gal staining (74.6±3.5%, number of slices=5). Neither calretinin-positive amacrine cells nor calbindin-D28k-positive amacrine cells exhibited β-gal staining (number of slices=5). Also, neither horizontal cells visualized using calbindin-D28k

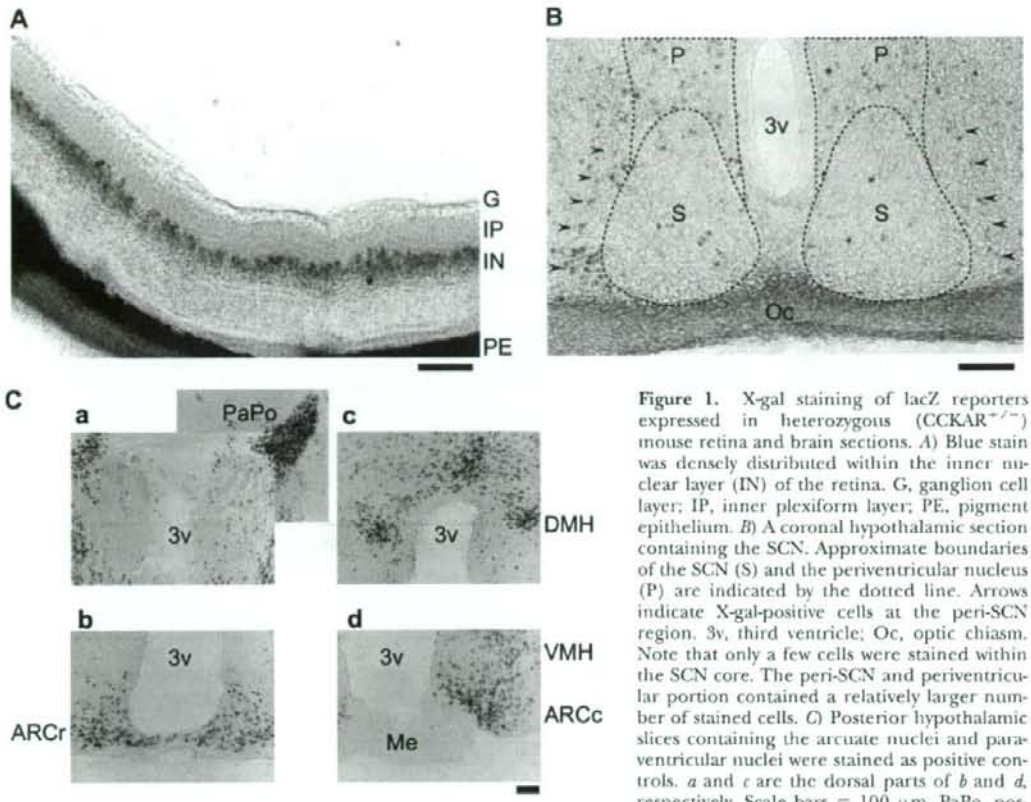

Figure 1. X-gal staining of lacZ reporters expressed in heterozygous ($CCKAR^{+/-}$) mouse retina and brain sections. *A*) Blue stain was densely distributed within the inner nuclear layer (IN) of the retina. G, ganglion cell layer; IP, inner plexiform layer; PE, pigment epithelium. *B*) A coronal hypothalamic section containing the SCN. Approximate boundaries of the SCN (S) and the periventricular nucleus (P) are indicated by the dotted line. Arrows indicate X-gal-positive cells at the peri-SCN region. 3v, third ventricle; Oc, optic chiasm. Note that only a few cells were stained within the SCN core. The peri-SCN and periventricular portion contained a relatively larger number of stained cells. *C*) Posterior hypothalamic slices containing the arcuate nuclei and paraventricular nuclei were stained as positive controls. *a* and *c* are the dorsal parts of *b* and *d*, respectively. Scale bars = 100 μm. PaPo, posterior paraventricular nucleus; ARCr, rostral arcuate nucleus; ARCc, caudal arcuate nucleus; Me, median eminence; DMH, dorsal medial hypothalamus; VMH, ventral medial hypothalamus.

staining nor bipolar cells visualized using Chx10 staining exhibited β-gal staining (number of slices=5). These results clearly indicate that CCK-A receptors were expressed specifically on amacrine cells, most of which also expressed glycine transporters.

Stimulation of CCK-A receptors mobilized intracellular Ca^{2+} in retinal amacrine cells but not in SCN neurons

We used Ca^{2+} imaging of organotypic cultures of retina and SCN to analyze the functional expression of CCK-A receptors within the photic input pathways to the circadian clock. First, Fura-2 AM-stained retinal cultures of wild-type (n=8), $CCKAR^{+/-}$ (n=8), and $CCKAR^{-/-}$ (n=8) mice were stimulated using the CCK-A receptor agonist, CCK-8s (300 nM, 1 min). CCK-8s evoked Ca^{2+} transients in 7.1 ± 1.8% of the Fura-2 AM-stained cells (total number of cells=234) in wild-type retina and 5.7 ± 1.9% of the cells (total number of cells=228) in $CCKAR^{+/-}$ retina (**Fig. 3*A*, *C***). These responding cells were identified as amacrine cells by the postexperimental X-gal staining of $CCKAR^{+/-}$ retina (Fig. 3*C*). The CCK-8s-induced Ca^{2+} transient but not the high K^+-induced Ca^{2+} flux was absent in $CCKAR^{-/-}$ retina (total number of cells=230) (Fig. 3*A*, *C*). The CCK-8s-induced Ca^{2+} transient observed in wild-type retina was significantly inhibited using the CCK-A antagonist, lorglumide (300 nM, application 5 min before the CCK-8s application; $F_{5,42}$=7.08, P<0.01 by one-way ANOVA followed by Duncan's multiple-range tests) (Fig. 3*C*). The CCK-8s-induced Ca^{2+} transients observed in wild-type retinas were resistant to the replacement of normal extracellular buffer with Ca^{2+}-free buffer (responding cell population=7.8±2.2%, total number of cells=215). CCK-8s-induced Ca^{2+} transients were completely eliminated, however, after thapsigargin-depletion of internal Ca^{2+} stores ($F_{5,42}$=7.08, P<0.01 by one-way ANOVA followed by Duncan's multiple-range tests) (Fig. 3*B*, *C*).

Second, organotypic slice cultures of SCN expressing a yellow cameleon 2.1 sensor linked to a neuron-specific enolase promoter were used to examine the effects of exposure to either CCK-8s or glutamate (**Fig. 4**). Within the core region, ~75% of cultured SCN neurons (55 of 73 neurons, number of slices=11) exhibited a significant increase in cytosolic Ca^{2+} in response to exposure to glutamate (300 μM, 1 min), but exhibited no response to CCK-8s (300 nM, 1 min) (Fig. 4*A*). A similar response to

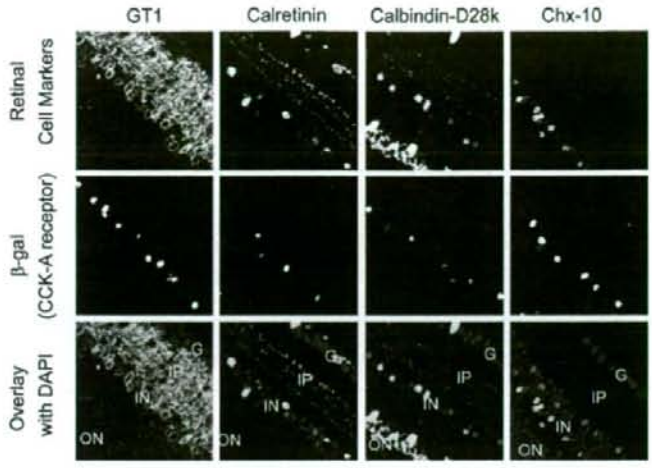

Figure 2. Immunofluorescent staining of heterozygous (CCKAR$^{+/-}$) mouse retina. The lacZ reporters stained with anti-β-gal antibody (middle row, shown as red in the bottom row), immunostaining for several retinal cell markers (top row, indicated above, shown as green in the bottom row), and counterstaining with DAPI (blue in the bottom row) were viewed and superimposed using a confocal scanning microscope. Anti-glycine transporter 1 (GT1) stains the plasma membrane of cell bodies and dendrites of glycinergic amacrine cells specifically. β-Gal staining strongly colocalized with GT1 staining of cell bodies (asterisks on the overlay image). Anti-calretinin antibody and/or anti-calbindin-D28k antibody recognizes another class of amacrine cells, horizontal cells, and/or ganglion cells, all of which did not colocalize with β-gal staining. Also, bipolar cells stained with anti-Chx10 antibody were not colocalized with β-gal stain. Scale bar = 50 μm. ON, outer nuclear layer; IN, inner nuclear layer; IP, inner plexiform layer; G, ganglion cell layer.

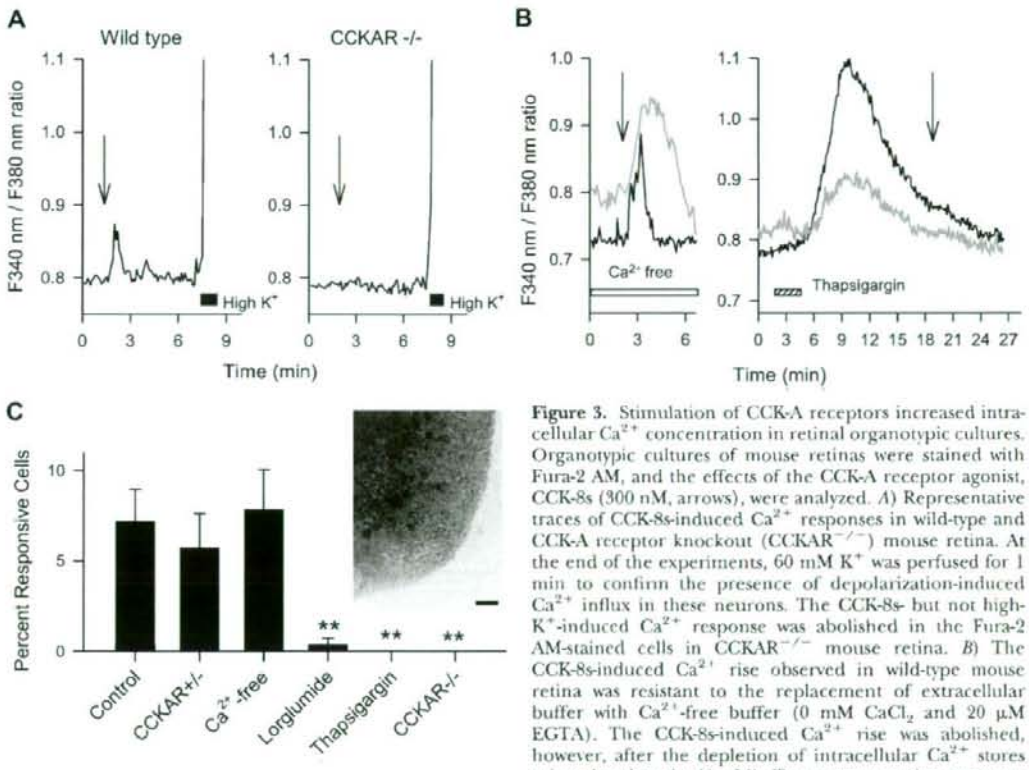

Figure 3. Stimulation of CCK-A receptors increased intracellular Ca^{2+} concentration in retinal organotypic cultures. Organotypic cultures of mouse retinas were stained with Fura-2 AM, and the effects of the CCK-A receptor agonist, CCK-8s (300 nM, arrows), were analyzed. *A*) Representative traces of CCK-8s-induced Ca^{2+} responses in wild-type and CCK-A receptor knockout (CCKAR$^{-/-}$) mouse retina. At the end of the experiments, 60 mM K^+ was perfused for 1 min to confirm the presence of depolarization-induced Ca^{2+} influx in these neurons. The CCK-8s- but not high-K^+-induced Ca^{2+} response was abolished in the Fura-2 AM-stained cells in CCKAR$^{-/-}$ mouse retina. *B*) The CCK-8s-induced Ca^{2+} rise observed in wild-type mouse retina was resistant to the replacement of extracellular buffer with Ca^{2+}-free buffer (0 mM $CaCl_2$ and 20 μM EGTA). The CCK-8s-induced Ca^{2+} rise was abolished, however, after the depletion of intracellular Ca^{2+} stores using thapsigargin (3 μM). Two representative responses from different cells (black and gray) are shown. *C*) Percentage of the retinal cells responding to CCK-8s. The CCK-A receptor antagonist, lorglumide (300 nM), also inhibited the CCK-8s-induced Ca^{2+} response. $^{**}P < 0.01$ by one-way ANOVA followed by Duncan's multiple-range tests. Inset: The CCK-8s-induced Ca^{2+} response was exclusively observed in amacrine cells, which were postexperimentally identified by X-gal (blue) staining in organotypic cultures of CCKAR$^{+/-}$ mouse retina. Scale bar = 100 μm.

glutamate was observed in slice cultures of CCKAR$^{-/-}$ mouse SCN (14 of 20 neurons, number of slices=3). Of a total of 73 neurons analyzed in the wild-type slice, one neuron in the dorsomedial periventricular region exhibited a sustained increase in cytosolic Ca^{2+} in response to CCK-8s, and this effect was completely inhibited in the presence of lorglumide (300 nM) (Fig. 4*B*). The amplitude of the glutamate response after exposure to CCK-8s was similar to that in the presence of lorglumide in this particular neuron.

Light pulse-induced *mPer1* and *mPer2* gene expression was reduced in the SCN of CCKAR$^{-/-}$ mice

To examine the effects of CCKAR$^{-/-}$ on light-induced responses of SCN neurons, we examined quantitative PCR for *mPer1* and *mPer2* mRNAs in SCN grafts. Under constant darkness conditions, the levels of *mPer1* and *mPer2* mRNAs oscillated in a circadian fashion both in the wild-type and CCKAR$^{-/-}$ SCN (**Fig. 5*A*, *B***). The approximate peaks of *mPer1* and *mPer2* occurred at identical times in the wild-type and CCKAR$^{-/-}$ SCN: at circadian time 6 for *mPer1* and at circadian time 9 for *mPer2* (Fig. 5*B*). Brief light pulse exposure (70 lux, 15 min) applied 4 h after the activity-onset time (circadian time 16), significantly increased the expression of *mPer1* (3.2-fold of unexposed control; $P<0.01$ by Student's *t* test) and *mPer2* (3.6-fold of unexposed control; $P<0.01$ by Student's *t* test) in the wild-type SCN (Fig. 5*C*). The light pulse-induced *mPer1* expression (1.6-fold of unexposed control; $P=0.16$ by Student's *t* test) and *mPer2* expression (1.7-fold of unexposed control; $P=0.09$ by Student's *t* test) were less evident in the SCN grafts of CCKAR$^{-/-}$ mice (Fig. 5*C*). The light pulse-induced increase in *mPer1* and *mPer2* mRNAs in wild-type SCN and the reduction in the responsiveness in the CCKAR$^{-/-}$ SCN were also visualized using *in situ* hybridization in SCN sections (Fig. 5*D*).

Light pulse-induced behavioral phase shifts and pupillary reflex were reduced in CCKAR$^{-/-}$ mice

Infrared sensor detection of activity/rest patterns across 24-h light-dark cycles (data not shown) and free-running periods of behavioral rhythms in constant darkness (**Fig. 6*A***) were almost identical between wild-type mice ($\tau=23.8\pm0.06$ h, $n=8$) and CCKAR$^{-/-}$ mice ($\tau=23.9\pm0.04$ h, $n=8$). The magnitude of behavioral phase delays caused by a light pulse exposure (10–500 lux for 15 min) at circadian time 16 was analyzed in wild-type and CCKAR$^{-/-}$ mice. Both types exhibited activity-onset delays depending on the intensity of light exposure (Fig. 6*B*). The magnitude of the phase delays caused by 50 lux or larger, however, was significantly smaller in CCKAR$^{-/-}$ mice than in wild-type mice. The maximal reduction in responsiveness was observed at 50 lux, at which CCKAR$^{-/-}$ mice exhibited a 42% smaller magnitude in phase shift than that of wild-type mice ($P<0.05$ by Student's *t* test, $n=8$ for both types). The maximal response at 500 lux was still 35% smaller in CCKAR$^{-/-}$ mice ($P<0.01$ by Student's *t* test, $n=8$ for both types) (Fig. 6*B*).

To examine the effects of CCKAR$^{-/-}$ on nonimage-forming visual functions, we further analyzed the consensual pupillary reflex using infrared video systems. The dark-adapted aperture areas were not significantly different between the wild-type mice (2.43 ± 0.07 mmϕ, $n=5$) and CCKAR$^{-/-}$ mice (2.48 ± 0.03 mmϕ, $n=4$). Also, atropine-induced aperture areas observed at the end

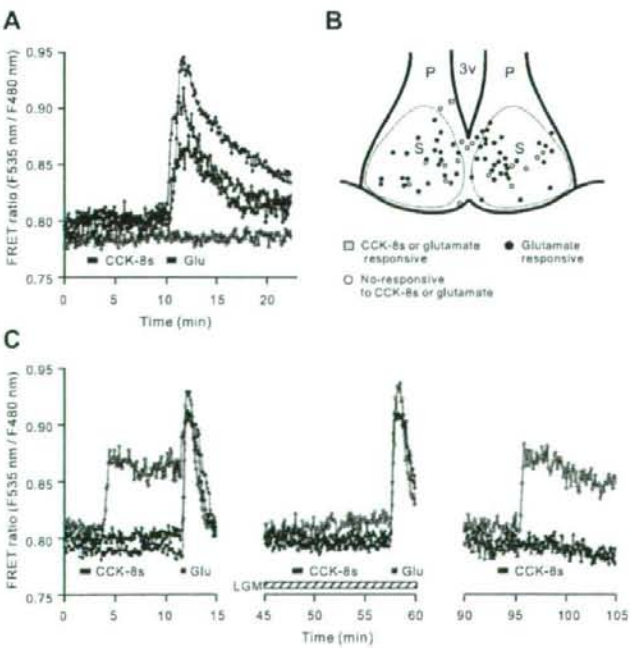

Figure 4. CCK-A receptors were not expressed in retino-recipient SCN neurons. Yellow cameleon 2.1 imaging of organotypic SCN cultures was used to investigate CCK-A receptor function in SCN neurons. A total of 73 neurons in wild-type SCN were exposed to CCK-8s (300 nM) followed by glutamate (Glu) (300 μM). *A*) Example cytosolic Ca^{2+} levels in four neurons. The cytosolic Ca^{2+} concentration increased in response to exposure to glutamate in three of four neurons shown. *B*) Approximate distribution of recorded neurons in the SCN (S) and the periventricular nucleus (P). Glutamate-induced Ca^{2+} responses were observed in neurons distributed throughout the SCN. CCK-8s did not mobilized cytosolic Ca^{2+} in 72 cells. 3v, third ventricle. *C*) One exception was found in the dorsomedial periventricular area (shown as a gray square in *B*), in which the cytosolic Ca^{2+} concentration increased in response to either CCK-8s or glutamate. The Ca^{2+} response to CCK-8s was inhibited by lorglumide (LGM) (300 nM).

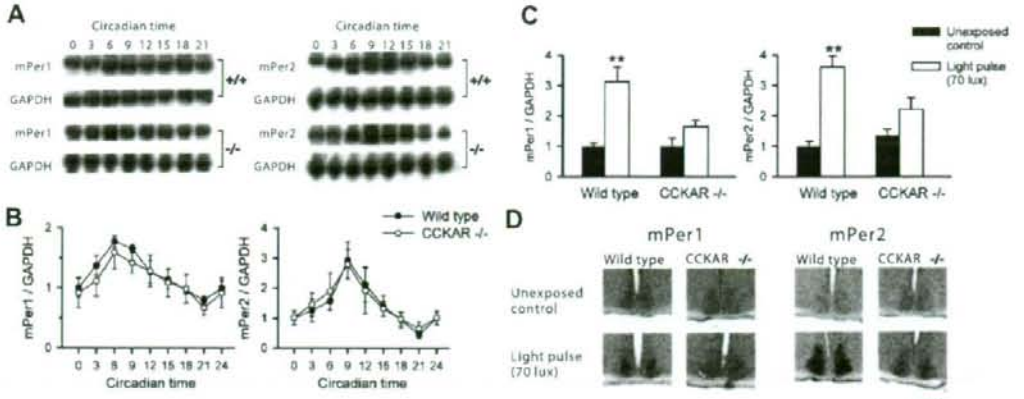

Figure 5. Light pulse-induced *mPer1* and *mPer2* gene expression was reduced in CCKAR$^{-/-}$ mice. *A*) Example blotting of *mPer1* and *mPer2* using wild-type SCN (+/+) and CCK-A receptor knockout SCN (−/−), both of which were sampled from mice maintained in constant darkness. *B*) *mPer1* and *mPer2* mRNA levels were quantified in terms of GAPDH mRNA levels. Circadian rhythms in *mPer1* and *mPer2* mRNA levels were observed in the SCN regardless of the genotypes. *C*) A light pulse (15 min, 70 lux) at circadian time 16 elevated *mPer1* and *mPer2* mRNA levels in the wild-type SCN sampled 60 min later. $^{**}P < 0.01$ by Student's *t* test. The light pulse-induced *mPer1* and *mPer2* mRNA expression was less evident in CCKAR$^{-/-}$ mice. $n = 4$ for each group. *D*) Topographical analysis of *mPer1* and *mPer2* mRNA expression in the SCN was also examined using *in situ* hybridization. The light pulse was applied as above to estimate the light-induced *mPer1* and *mPer2* mRNA expression in the SCN. Scale bar = 500 μm.

of experiments were not significantly different between the wild-type mice (2.60±0.08 mmϕ, n=5) and CCKAR$^{-/-}$ mice (2.67±0.09 mmϕ, n=4). The irradiance-dependent pupillary constrictions caused by 20, 100, or >1000 lux light were also observed both for the wild-type mice ($F_{2,92}$=440.2, P<0.01 by two-way ANOVA) and CCKAR$^{-/-}$ mice ($F_{2,92}$=183.9, P<0.01 by two-way ANOVA for the wild-type group) (**Fig. 7A**). However, the minimal pupillary dimensions followed by exposures of 100-lux light (+64.7%; P<0.05 by Student's *t* test) or >1000-lux light (+154.3%; P<0.05 by Student's *t* test) were significantly larger in CCKAR$^{-/-}$ mice (Fig. 7*B*, *C*).

DISCUSSION

The results of the present study demonstrate that in mice there is robust expression of CCK-A receptors on retinal glycinergic amacrine cells, with relatively little expression on SCN neurons that receive projections from the retina. Also, a CCK-A agonist induced intracellular Ca^{2+} mobilization in amacrine cells and not SCN neurons. Moreover, mutant mice deficient in CCK-A receptors exhibited reduced light pulse-induced *mPer1*/*mPer2* gene expression in the SCN. Furthermore, light pulse-induced behavioral phase shifts and pupillary reflex were also significantly reduced in CCKAR$^{-/-}$ mice. Taken together, these data indicate that functional CCK-A receptors located primarily on amacrine cells are the most significant cause for circadian modulation of *mPer1*/*mPer2* gene expression in the SCN and can modulate nonimage-forming visual functions. Thus, we suggest a novel function of CCK-A receptors in retinal signal processing.

Little CCK function in retino-recipient SCN neurons

CCK peptides have previously been reported to be expressed to some degree in SCN neurons (6, 15–17), so we carefully analyzed the possible functionality of CCK-A receptors in SCN neurons. X-gal stained only sparsely scattered cells in the SCN, with a rather denser distribution in the peri-SCN and periventricular zones. Consistent with this result, our Ca^{2+} imaging studies in organotypic SCN cultures demonstrated that core SCN neurons did not respond to the CCK-A receptor agonist, CCK-8s. An increase in cytosolic Ca^{2+} evoked by either CCK-8s or glutamate was observed in only one neuron located in the periventricular region, where retino-recipient neurons are absent or rare (16). Although lack of CCK-8s effects on glutamate receptive SCN neurons may be due to limitations of samples in our Ca^{2+} imaging studies, this result is consistent with the reported distribution of CCK peptides in the mouse, because dorsal efferent fibers from the SCN but not retinohypothalamic tracts are CCK-immunoreactive in mice (16). Therefore, CCK peptides may have a role in the efferent transmission from SCN neurons and/or transmission between intra-SCN neurons but not for transmission to retino-recipient SCN neurons.

Because CCK is one of the most abundant neuropeptides in the brain, and several brain loci responsible for visual input, such as the dorsal lateral geniculate, express CCK-A receptors (33), careful discussion is needed to identify the localization of CCK-A receptors responsible for the modulation of nonimage-forming visual functions. The SCN receive geniculohypothalamic tracts (GHT) from the intergeniculate leaflet (IGL) of the thalamus (6). It has been shown that the GHT uses neuropeptide-Y and GABA as neurotransmitters to the SCN, and this pathway is involved in the

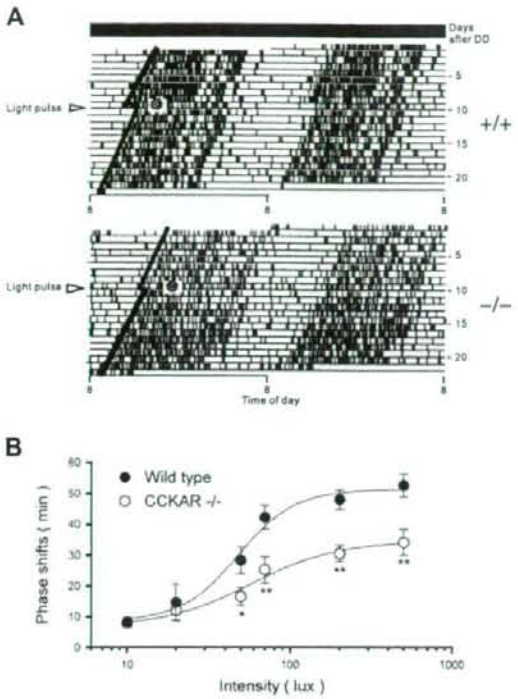

Figure 6. Light pulse-induced behavioral phase shifts were reduced in CCKAR$^{-/-}$ mice. *A*) Representative double-plot actograms showing circadian phase delays in response to a light pulse (15 min, 50 lux) in a wild-type mouse (+/+) and a CCKAR$^{-/-}$ mouse (−/−). Double circles denote the timing of the light pulse exposure at circadian time 16. The approximate activity-onset time is indicated on the left-hand actograms (lines fitted by eye). *B*) Irradiation response curve for the circadian phase shifts evoked by a 15-min light pulse applied at circadian time 16. Although both genotypes exhibited an intensity-dependent increase in the magnitude of the phase shifts, CCKAR$^{-/-}$ mice exhibited shorter circadian phase delays when the light pulse was more intense than 50 lux. $n = 4$–11 in each group. $^{*}P < 0.05$ and $^{**}P < 0.01$ in comparison with the corresponding wild-type group by Student's t test.

behavioral phase shifts *via* nonphotic inputs, such as that *via* activity elevations and triazolam administrations (6). Also, it has been shown that a free running period during constant light is reduced by IGL lesions, and thus the GHT pathway may be involved in the tonic effects of light (6). However, to our knowledge, there have been no reports showing that light pulse-induced phase shifts are significantly modulated by IGL lesions in mice. Whether CCK-A receptors are expressed on any of the GHT pathways to the SCN is currently not known; therefore, it is reasonable to consider that significant reduction of photoentrainment in CCKAR$^{-/-}$ mice is due to the modulation of reticulohypothalamic (RHT) pathways not of GHT pathways. Within the RHT pathways, the results of the lacZ reporter assays and Ca^{2+} imaging in the present study suggest that the principal site of CCK-A receptor actions for circadian photoentrainment is confined within the retina not in SCN neurons.

Possible function of CCK-A receptors in mouse amacrine cells

Approximately 30 different types of amacrine cells have been identified in the mammalian retina (34). About half of the amacrine cells contain GABA and the other half contain glycine as inhibitory neurotransmitters, and both of these types of amacrine cells express ionotropic glutamate receptors to receive glutamatergic input from bipolar cells (35). Despite the abundant knowledge about the morphological diversity of amacrine cells, their physiological functions are poorly understood, especially at a systems level. One of the best characterized functions is inhibitory neurotransmission on the synapse between bipolar cells and retinal ganglion cells (36). This amacrine cell function contributes to the transient firing pattern of retinal ganglion cells, which is required for background control for motion perception (37, 38). The present results suggest that amacrine cells have a novel role in circadian photoentrainment, because *1*) CCK-A receptors were concentrated on glycine transporter-positive amacrine cells but not on retino-recipient SCN neurons, *2*) a CCK-A receptor agonist evoked calcium responses in amacrine cells of wild-type but not of CCKAR$^{-/-}$ mice nor in the SCN of wild-type mice, *3*) CCKAR$^{-/-}$ mice exhibited reduced light pulse-induced *mPer1/mPer2* expression in the SCN, and *4*) CCKAR$^{-/-}$ mice exhibited reduced light pulse-induced behavioral phase shifts. Notably, these results suggest that CCK-A receptor activation results in an excitatory effect on retinal ganglion cells that project to the SCN, because the photic response of the SCN was significantly reduced in CCKAR$^{-/-}$ mice.

The present results showed that the cytosolic Ca^{2+} concentration was increased by CCK-8s in cultured amacrine cells. Activation of phospholipase C with generation of inositol 1,4,5-trisphosphate and diacylglycerol, subsequent Ca^{2+} release from internal Ca^{2+} stores, and activation of protein kinase C is the proposed intracellular signaling common to a wide variety of cells after CCK-A receptor activation (39–41). Accordingly, the CCK-8s-induced Ca^{2+} response in cultured amacrine cells remained in Ca^{2+}-free extracellular medium but was abolished by the depletion of internal Ca^{2+} stores by thapsigargin. In chick retinal cultures, protein kinase Cγ colocalizes with α-amino-3-hydroxy-5-methyl-4-isoxazole-propionic acid (AMPA) -type glutamate receptors, and phosphorylation of AMPA receptors by protein kinase C causes translocation of AMPA receptors to the plasma membrane and increases excitatory synaptic transmission (42). Axons from glycinergic amacrine cells have been reported to terminate on neighboring GABAergic amacrine cells, which terminate on the synapse between bipolar cells and retinal ganglion cells (38). Therefore, one possible explanation of the excitatory action of CCK-A receptor activation on the ON bipolar-ganglion cell synapse is that activation of CCK-A receptors excites glycinergic amacrine cells, which inhibit GABAergic amacrine

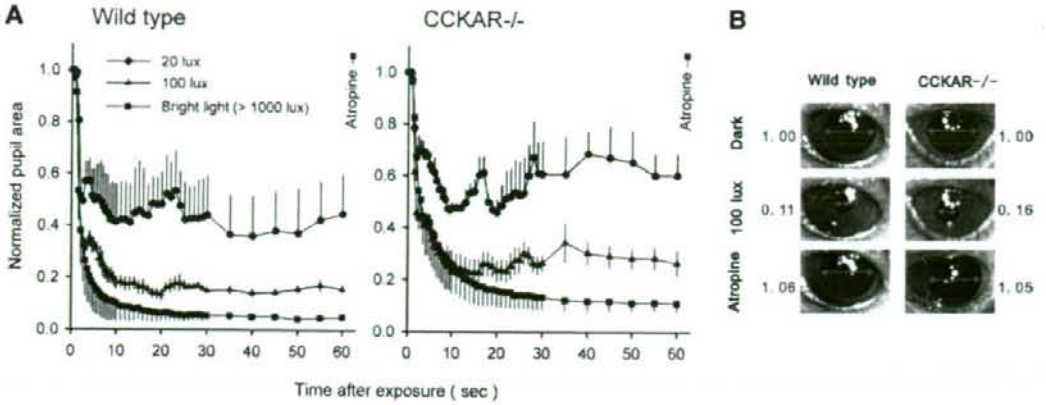

Figure 7. Mice lacking CCK-A receptors exhibit an incomplete pupillary light reflex. *A*) Time course changes in the normalized pupil area during light exposure at different intensities (20, 100, or >1000 lux). All of these light exposures were followed by 1–2 h dark adaptation during the daytime. The dark-adapted aperture area just before light exposure was regarded as 1.0. The maximal aperture area was estimated by an atropine instillation at the end of experiments. Note that irradiation-dependent pupillary reflex was observed for both genotypes, but CCKAR$^{-/-}$ mice displayed reduced pupillary constriction compared with the wild-type mice. *B*) Example video frames taken in the session of 100-lux irradiation. Pupil diameters (r) were estimated as arrows. Relative size of pupillary area was calculated based on r^2 of dark-adapted pupil image. *C*) The minimal pupil area during 1 min of light exposure was significantly larger in CCKAR$^{-/-}$ mice than in the wild-type mice when they were exposed at 100 lux or >1000 lux. $n = 4$–5 in each group. $^*P < 0.05$ by Student's t test.

cells. Inhibition of GABAergic amacrine cells would then disinhibit the bipolar ganglion cell synapse. Retinal ganglion cells, which project to the SCN, could then be activated by ON bipolar cell activity (**Fig. 8**). It is also possible that the excitation of glycinergic amacrine cells by activation of CCK-A receptors may inhibit OFF bipolar terminals, which may also allow activation of retinal ganglion cells. It has been suggested, however, that intrinsically photosensitive retinal ganglion cells, which are the predominant type (~75%) of SCN-projecting retinal ganglion cells (43) only receive ON bipolar terminals and amacrine cell terminals (8).

Rhythmic *mPer1* expression has been reported to occur in the majority of GABAergic amacrine cells but not glycinergic amacrine cells (44). Also, the AII amacrine cells exhibit circadian rhythms in parvalbumin expression in constant darkness (45). Therefore, a subpopulation of amacrine cells may contain an intrinsic molecular clock mechanism. It has not been shown previously, however, that amacrine cell-mediated pathways have a critical role in circadian photoentrainment. The present results showed that CCKAR$^{-/-}$ mice exhibited significantly reduced bright light-induced behavioral phase shifts; thus, we propose that the CCK-A receptor-mediated amacrine cell pathway has an important role in circadian photoentrainment *via* cone photoreceptor pathways, although we cannot exclude the possible involvement of rods in this signaling pathway only with the results of behavioral phase shifts. In specific photoreceptor-deficient mutants, such as midwavelength coneless mice (46), exposure to full-spectrum light or saturating bright light (>100 lux) masks their deficiency in circadian photoentrainment. In the present study, however, CCKAR$^{-/-}$ mice exhibited a significantly reduced saturating bright light response, suggesting that multiple cone-mediated pathways may be processed *via* amacrine cells that express CCK-A receptors. This hypothesis is consistent with the dense lateral distribution of CCK-A receptors within the inner nuclear layer that we observed in the present study using X-gal staining.

CCK-A receptors may control outputs and inputs of the circadian clock

The present data show that CCK-A receptors are involved in the photic input to the SCN for photoentrainment. This finding raises the possibility that CCK receptors in related structures may have additional functions in other aspects of circadian control of behaviors. For example, the CCK peptide is known as an important regulator for feeding behaviors, and CCK-A receptors may participate in control of satiety both *via* central and gastrointestinal systems (47). As described above, efferent fibers from the SCN contain CCK peptides (16), and they may terminate on satiety-controlling hypothalamic nuclei such as the paraventricular nucleus and dorsal medial hypothalamus that express CCK-A receptors (47), observable also in our results (Fig. 1). This suggestion raises the possibility that CCK outputs from the SCN contribute to the circadian rhythms in feeding behaviors. If so, the CCK-A receptor-mediated pathway could not be the sole output from the SCN because CCKAR$^{-/-}$ mice maintain normal nocturnal feeding rhythms (48). Consistent with this hypothesis,

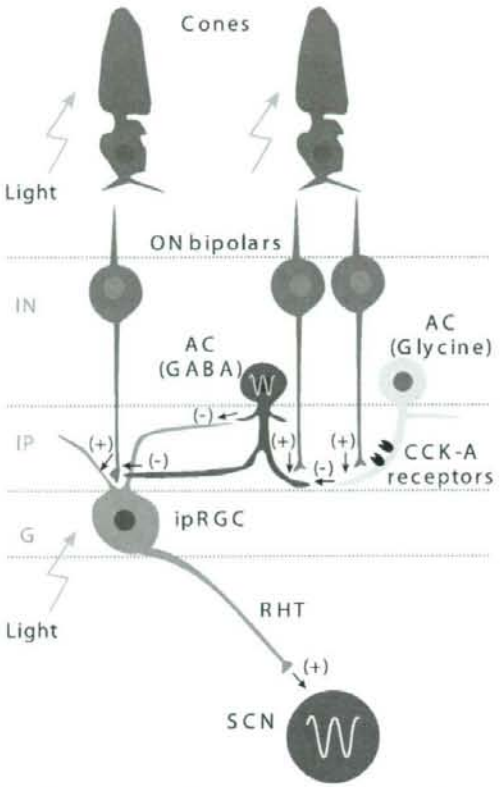

Figure 8. Diagram of the possible retinal circuitry underlying the role of amacrine cells and CCK-A receptors in photoentrainment of the circadian clock. Activation of CCK-A receptors excites glycinergic amacrine cells [AC (Glycine)]. These cells may then inhibit activation of GABAergic amacrine cells [AC (GABA)], which would disinhibit ON bipolar-ganglion cell synapses, allowing activation of intrinsically photosensitive retinal ganglion cells (ipRGC) and then SCN neurons. We propose that glycinergic amacrine cells modulate cone-mediated pathways because CCKAR$^{-/-}$ mice exhibited significantly reduced phase shifts in response to bright light pulses and functional CCK-A receptors were located primarily on glycinergic amacrine cells. Sine waves indicate cell types in which intrinsic intracellular clock gene oscillations have been described (GABAergic amacrine cells and SCN neurons). IN, inner nuclear layer; IP, inner plexiform layer; G, ganglion cell layer; RHT, retinohypothalamic tract. (+) denotes excitatory synaptic transmission, and (−) denotes inhibitory synaptic transmission in the presence of light.

our locomotor activity recordings also showed strong circadian rhythms in CCKAR$^{-/-}$ mice.

We have previously observed that light pulse-induced phase shifts and *c-fos* expression in the SCN were reduced in obese mutant OLETF rats (26, 27), which lack multiple genes, including genes encoding CCK-A receptors (28, 29). The present study further demonstrated that CCKAR$^{-/-}$ mice exhibited impaired circadian photoentrainability similar to that observed in OLETF rats. The CCKAR$^{-/-}$ mice are not obese, presumably due to the basal energy balance of mice, although food intake activity is up-regulated in mutant mice (30, 48, 49). Therefore, a lack of CCK-A receptors, but not an obese phenotype, underlies impaired circadian photoentrainability. The present study demonstrated that in CCKAR$^{-/-}$ mice a key cause of impaired photoentrainability is a deficiency in CCK-A receptor expression in amacrine cells.

As in cerebral CCK-receptive neurons, amacrine cells may receive CCK peptides from neighboring retinal neurons, because CCK peptides have been found in retina (18–22), and blood-retinal barriers may prevent peptide transport from the gastrointestinal system. It has recently been suggested, however, that there may be direct regulation of satiety control centers by peripheral nutritional signals, such as CCK, ghrelin, and leptin, *via* "leaky" portions of the blood-brain barrier and circumventricular organs (47, 50). This suggestion raises the possibility that peripheral CCK harmonistically activates cerebral and retinal CCK-A receptors, adding an interesting aspect to possible circadian clock mechanisms, especially at a systems level and in relation to metabolic control.

In conclusion, our data suggest a novel function for retinal CCK in nonimage-forming visual functions, including circadian photoentrainment and pupillary light reflex. CCK-A receptors on glycinergic amacrine cells may have a key role in the process of photoentrainment, probably modulating retinal ganglion cell activation of the SCN.

We thank Mr. Tomoya Ozaki (University of Toyama) for his assistance with the pupillary reflex recordings and Dr. Hitoshi Okamura (Kobe University) for kindly donating *mPer1* and *mPer2* probes for the *in situ* hybridization studies. We also thank Drs. David W. Marshak (University of Texas Medical School) and Charles N Allen (Oregon Health & Science University) for helpful comments and discussions on the manuscript. This work was supported in part by grants-in-aid for scientific research (16300104, 17659070, and 18021012) from the Ministry of Education, Culture, Sports, Science and Technology Japan to M.I. and a grant from the Naito Foundation to M.I. and T.S.

REFERENCES

1. Moore, R. Y., and Eichler, V. B. (1972) Loss of a circadian adrenal corticosterone rhythm following suprachiasmatic lesions in the rat. *Brain Res.* **42,** 201–206
2. Stephan, F. K., and Zucker, I. (1972) Circadian rhythms in drinking behavior and locomotor activity of rats are eliminated by hypothalamic lesions. *Proc. Natl. Acad. Sci. U. S. A.* **69,** 1583–1586
3. Freedman, M. S., Lucas, R. J., Soni, B., von Schantz, M., Munoz, M., David-Gray, Z., and Foster, R. (1999) Regulation of mammalian circadian behavior by non-rod, non-cone, ocular photoreceptors. *Science* **284,** 502–504
4. Berson, D. M., Dunn, F. A., and Takao, M. (2002) Phototransduction by retinal ganglion cells that set the circadian clock. *Science* **295,** 1070–1073
5. Lucas, R. J., Hattar, S., Takao, M., Berson, D. M., Foster, R. G., and Yau, K-W. (2003) Diminished pupillary light reflex at high irradiances in melanopsin-knockout mice. *Science* **299,** 245–247
6. Morin, L. P., and Allen, C. N. (2006) The circadian visual system, 2005. *Brain Res. Rev.* **51,** 1–60
7. Panda, S., Provencio, I., Tu, D. C., Pires, S. S., Rollag, M. D., Castrucci, A. M., Pletcher, M. T., Sato, T. K., Wiltshire, T., Andahazy, M., Kay, S. A., Van Gelder, R. N., and Hogenesch,

J. B. (2003) Melanopsin is required for non-image-forming photic responses in blind mice. *Science* **301,** 525–527
8. Belenky, M. A., Smeraski, C. A., Provencio, I., Sollars, P. J., and Pickard, G. E. (2003) Melanopsin retinal ganglion cells receive bipolar and amacrine cell synapses. *J. Comp. Neurol.* **460,** 380–393
9. Ding, J. M., Chen, D., Weber, E. T., Faiman, L. E., Rea, M. A., and Gillette, M. U. (1994) Resetting the biological clock: mediation of nocturnal circadian shifts by glutamate and NO. *Science* **266,** 1713–1717
10. Shearman, L. P., Zylka, M. J., Weaver, D. R., Kolakowski, L. F., and Reppert, S. M. (1997) Two period homologs: circadian expression and photic regulation in the suprachiasmatic nuclei. *Neuron* **19,** 1261–1269
11. Ikeda, M. (2004) Calcium dynamics and circadian rhythms in suprachiasmatic nucleus neurons. *Neuroscientist* **10,** 315–324
12. Hannibal, J. (2002) Neurotransmitters of the retino-hypothalamic tract. *Cell Tissue Res.* **309,** 73–88
13. Pickard, G. E., Smith, B. N., Belenky, M., Rea, M. A., Dudek, F. E., and Sollars, P. J. (1999) 5-HT1B receptor-mediated presynaptic inhibition of retinal input to the suprachiasmatic nucleus. *J. Neurosci.* **19,** 4034–4045
14. Moldvan, M. G., Irwin, R. P., and Allen, C. N. (2006) Presynaptic $GABA_B$ receptors regulate retinohypothalamic tract synaptic transmission by inhibiting voltage-gated Ca^{2+} channels. *J. Neurophysiol.* **95,** 3727–3741
15. Van den Pol, A. N., and Tsujimoto, K. L. (1985) Neurotransmitters of the hypothalamic suprachiasmatic nucleus: immunocytochemical analysis of 25 neuronal antigens. *Neuroscience* **15,** 1049–1086
16. Silver, R., Sookhoo, A. I., LeSauter, J., Stevens, P., Jansen, H. T., and Lehman, M. N. (1999) Multiple regulatory elements result in regional specificity in circadian rhythms of neuropeptide expression in mouse SCN. *Neuroreport* **10,** 3165–3174
17. LeSauter, J., Kriegsfeld, L. J., Hon, J., and Silver, R. (2002) Calbindin-D_{28K} cells selectively contact intra-SCN neurons. *Neuroscience* **111,** 575–585
18. Osborne, N. N., Nicholas, D. A., Cuello, A. C., and Dockray, G. J. (1981) Localization of cholecystokinin immunoreactivity in amacrine cells of the retina. *Neurosci. Lett.* **26,** 31–35
19. Eskay, R. L., and Beinfeld, M. C. (1982) HPLC and RIA of cholecystokinin peptides in the vertebrate neural retina. *Brain Res.* **246,** 315–318
20. Osborne, N. N., Nicholas, D. A., Dockray, G. J., and Cuello, A. C. (1982) Cholecystokinin and substance P immunoreactivity in retinas of rats, frogs, lizards, and chicks. *Exp. Eye Res.* **34,** 639–649
21. Marshak, D. W., Aldrich, L. B., Valle, J. D., and Yamada, T. (1990) Localization of immunoreactive cholecystokinin precursor to amacrine cells and bipolar cells of the macaque monkey retina. *J. Neurosci.* **10,** 3045–3055
22. Firth, S. L., Varela, C., de la Villa, P., and Marshak, D. (2002) Cholecystokinin-like immunoreactive amacrine cells in the rat retina. *Vis. Neurosci.* **19,** 531–540
23. Bragado, M. J., Perez-Marquez, J., and Garcia-Marin, L. J. (2003) The cholecystokinin system in the rat retina: receptor expression and in vivo activation of tyrosine phosphorylation pathways. *Neuropeptides* **37,** 374–380
24. Funakoshi, A., Miyasaka, K., Shinozaki, H., Masuda, M., Kawanami, T., Takata, Y., and Kono, A. (1995) An animal model of congenital defect of gene expression of cholecystokinin (CCK)-A receptor. *Biochem. Biophys. Res. Commun.* **210,** 787–796
25. Takiguchi, S., Takata, Y., Funakoshi, A., Miyasaka, K., Kataoka, K., Fujimura, Y., Goto, T., and Kono, A. (1997) Disrupted cholecystokinin type-A receptor (CCKAR) gene in OLETF rats. *Gene* **197,** 169–175
26. Yamanouchi, S., Shimazoe, T., Nagata, S., Moriya, T., Maetani, M., Shibata, S., Watanabe, S., Miyasaka, K., Kono, A., and Funakoshi, A. (1997) Decreased level of light-induced Fos expression in the suprachiasmatic nucleus of diabetic rats. *Neurosci. Lett.* **227,** 103–106
27. Shimazoe, T., Maetani, M., Nakamura, S., Yamanouchi, S., Watanabe, S., Miyasaka, K., Kono, A., and Funakoshi, A. (1999) Lowered entrainment function in the suprachiasmatic nucleus of Otsuka Long Evans Tokushima Fatty (OLETF) rats. *Jpn. J. Pharmacol.* **80,** 85–88
28. Ogino, T., Wei, S., Wei, K., Moralejo, D. H., Kose, H., Mizuno, A., Shima, K., Sasaki, Y., Yamada, T., and Matsumoto, K. (2000) Genetic evidence for obesity loci involved in the regulation of body fat distribution in obese type 2 diabetes rat, OLETF. *Genomics* **70,** 19–25
29. Muramatsu, Y., Yamada, T., Taniguchi, Y., Ogino, T., Kose, H., Matsumoto, K., and Sasaki, Y. (2005) *Pnlip* encoding pancreatic lipase is possible candidate for obesity QTL in the OLETF rat. *Biochem. Biophys. Res. Commun.* **331,** 1270–1276
30. Takiguchi, S., Suzuki, S., Sato, Y., Kanai, S., Miyasaka, K., Jimi, A., Shinozaki, H., Takata, Y., Funakoshi, A., Kono, A., Minowa, O., Kobayashi, T., and Noda, T. (2002) Role of CCK-A receptor for pancreatic function in mice: a study in CCK-A receptor knockout mice. *Pancreas* **24,** 276–283
31. Hatakeyama, J., and Kageyama, R. (2002) Retrovirus-mediated gene transfer to retinal explants. *Methods* **28,** 387–395
32. Ikeda, M., Sugiyama, T., Wallace, C. S., Gompf, H. S., Yoshioka, T., Miyawaki, A., and Allen, C. N. (2003) Circadian dynamics of cytosolic and nuclear Ca^{2+} in single suprachiasmatic nucleus neurons. *Neuron* **38,** 253–263
33. Davidowa, H., Albrecht, D., Gabriel, H. J., and Zippel, U. (1995) Cholecystokinin affects the neuronal discharge mode in the rat lateral geniculate body. *Brain Res. Bull.* **36,** 533–537
34. MacNeil, M. A., and Masland, R. H. (1998) Extreme diversity among amacrine cells: implications for function. *Neuron* **20,** 971–982
35. Dumitrescu, O. N., Protti, D. A., Majumdar, S., Zeilhofer, H. U., and Wässle, H. (2005) Ionotropic glutamate receptors of amacrine cells of the mouse retina. *Vis. Neurosci.* **23,** 79–90
36. Wässle, H., and Boycott, B. B. (1991) Functional architecture of the mammalian retina. *Physiol. Rev.* **71,** 447–480
37. Nirenberg, S., and Meister, M. (1997) The light response of retinal ganglion cells is truncated by a displaced amacrine circuit. *Neuron* **18,** 637–650
38. Lagnado, L. (1998) Retinal processing: amacrine cells keep it short and sweet. *Curr. Biol.* **8,** R598–R600
39. Williams, J. A. (2001) Intracellular signaling mechanisms activated by cholecystokinin-regulating synthesis and secretion of digestive enzymes in pancreatic acinar cells. *Annu. Rev. Physiol.* **63,** 77–97
40. Herness, S., Zhao, F. L., Lu, S. G., Kaya, N., and Shen, T. (2002) Expression and physiological actions of cholecystokinin in rat taste receptor cells. *J. Neurosci.* **22,** 10018–10029
41. Simasko, S. M., Wiens, J., Karpiel, A., Covasa, M., and Ritter, R. C. (2002) Cholecystokinin increases cytosolic calcium in a subpopulation of cultured vagal afferent neurons. *Am. J. Physiol.* **283,** R1303–R1313
42. Correia, S. S., Duarter, C. B., Faro, C. J., Pires, E. V., and Carvalho, A. L. (2003) Protein kinase Cγ associates directly with the GluR4 α-amino-3-hydroxy-5-methyl-4-isoxazole propionate receptor subunit: effect on receptor phosphorylation. *J. Biol. Chem.* **278,** 6307–6313
43. Gooley, J. J., Lu, J., Chou, T. C., Scammell, T. E., and Saper, C. B. (2001) Melanopsin in cells of origin of the retinohypothalamic tract. *Nat. Neurosci.* **4,** 1165
44. Zhang, D. Q., Zhou, T., Ruan, G. X., and McMahon, D. G. (2005) Circadian rhythm of Period1 clock gene expression in NOS amacrine cells of the mouse retina. *Brain Res.* **1050,** 101–109
45. Gábriel, R., Lesauter, J., Bánvölgyi, T., Petrovics, G., Silver, R., and Witkovsky, P. (2004) All amacrine neurons of the rat retina show diurnal and circadian rhythms of parvalbumin immunoreactivity. *Cell Tissue Res.* **315,** 181–186
46. Dkhissi-Benyahya, O., Gronfier, C., Vanssay, W. D., Flamant, F., and Cooper, H. M. (2007) Modeling the role of mid-wavelength cones in circadian responses to light. *Neuron* **53,** 677–687
47. Fry, M., Hoyda, T. D., and Ferguson, A. V. (2007) Making sense of it: roles of the sensory circumventricular organs in feeding and regulation of energy homeostasis. *Exp. Biol. Med.* **232,** 14–26
48. Kopin, A. S., Mathes, W. F., McBride, E. W., Nguyen, M., Al-Haider, W., Schmitz, F., Bonner-Weir, S., Kanarek, R., and Beinborn, M. (1999) The cholecystokinin-A receptor mediates inhibition of food intake yet is not essential for the maintenance of body weight. *J. Clin. Invest.* **103,** 383–391
49. Bi, S., Scott, K. A., Kopin, A. S., and Moran, T. H. (2004) Differential roles for cholecystokinin A receptors in energy balance in rats and mice. *Endocrinology* **145,** 3873–3880
50. Jobst, E. E., Enriori, P. J., and Cowley, M. A. (2004) The electrophysiology of feeding circuits. *Trends Endocrinol. Metab.* **15,** 488–499

Received for publication August 2, 2007.
Accepted for publication November 15, 2007.

Neuroscience 151 (2008) 120–128

THE OLFACTORY CONDITIONING IN THE EARLY POSTNATAL PERIOD STIMULATED NEURAL STEM/PROGENITOR CELLS IN THE SUBVENTRICULAR ZONE AND INCREASED NEUROGENESIS IN THE OLFACTORY BULB OF RATS

K. SO,[a,b] T. MORIYA,[a] S. NISHITANI,[a] H. TAKAHASHI[b] AND K. SHINOHARA[a]*

[a]*Department of Neurobiology and Behavior, Unit of Basic Medical Sciences, Course of Medical and Dental Sciences, Nagasaki University Graduate School of Biomedical Sciences, 1-12-4 Sakamoto, Nagasaki 852-8523, Japan*

[b]*Department of Otolaryngology–Head and Neck Surgery, Unit of Translational Medicine, Course of Medical and Dental Sciences, Nagasaki University Graduate School of Biomedical Sciences, 1-7-1 Sakamoto, Nagasaki 852-8501, Japan*

Abstract—The olfactory memory acquired during the early postnatal period is known to be maintained for a long period, however, its neural mechanism remains to be clarified. In the present study, we examined the effect of olfactory conditioning during the early postnatal period on neurogenesis in the olfactory bulb of rats. Using the bromodeoxyuridine–pulse chase method, we found that the olfactory conditioning, which was a paired presentation of citral odor (conditioned stimulus) and foot shock (unconditioned stimulus) in rat pups on postnatal day 11, stimulated the proliferation of neural stem/progenitor cells in the anterior subventricular zone (aSVZ), but not in the olfactory bulb, at 24 h after the conditioning. However, the number of newborn cells in the olfactory bulb was increased at 2 weeks, but not 8 weeks, after such conditioning. Neither the exposure of a citral odor alone nor foot shock alone affected the proliferation of neural stem/progenitor cells in the aSVZ at 24 h after and the number of newborn cells in the olfactory bulb at 2 weeks after. The majority of newborn cells in the olfactory bulb of either the conditioned rats or the unconditioned rats expressed the neural marker NeuN, thus indicating that the olfactory conditioning stimulated neurogenesis in the olfactory bulb. These results suggest that olfactory conditioning during the early postnatal period temporally stimulates neurogenesis in the olfactory bulb of rats. © 2008 IBRO. Published by Elsevier Ltd. All rights reserved.

Key words: neural stem cells, proliferation, SVZ, bromodeoxyuridine, olfactory memory.

The olfactory function is well known to play an important role in the survival of newborn animals as well as in humans. The long-term olfactory memory acquired during the early postnatal period is involved in these olfactory functions, and therefore they are able to learn their mother's odor and successfully approach her nipple without any visual information (Teicher and Blass, 1976). In general, the paired presentation of odor and somatosensory stimulation is known to be crucial in establishing olfactory learning. In rat pups, the pairing of odor and foot shock is able to establish olfactory learning (Okutani et al., 1999; Sullivan et al., 2000). Okutani et al. (1999) have reported that rat pups that had been exposed to citral odor associated with shock treatment on postnatal day (PD) 11, showed an aversive response to that odor. At present, the mechanism underlying the olfactory learning in early postnatal rats is considered to involve the modulation and plasticity of the synapse in the olfactory bulb (Wilson and Sullivan, 1994; Sullivan and Wilson, 2003), which involves either GABA (Okutani et al., 1999, 2003), noradrenaline (Sullivan et al., 1989, 1992; Yuan et al., 2003) or serotonin (Yuan et al., 2003).

On the other hand, recent studies have revealed that the neural stem/progenitor cells, which possess the ability of proliferation and differentiation into neurons and glial cells (Ono et al., 2001), are located not only in the embryonic brain but also in the postnatal brain, including the anterior subventricular zone (aSVZ), subgranular zone of the hippocampal dentate gyrus (Gage, 2002) and the olfactory bulb (Fukushima et al., 2002; Gritti et al., 2002). The neural stem/progenitor cells in the aSVZ have been proven to migrate via the rostral migratory stream (RMS) and finally differentiate into interneurons, such as granule cells and periglomerular cells in the olfactory bulb, and it takes approximately 2 weeks for neural stem/progenitor cells to migrate and differentiate in the olfactory bulb (Altman, 1969; Luskin, 1993; Lois and Alvarez-Buylla, 1994; Kato et al., 2001; Coskun and Luskin, 2002). Furthermore, the proliferative and differentiative activities of the neural stem/progenitor cells in the aSVZ dynamically change under various physiological conditions such as pregnancy (Shingo et al., 2003) and enriched odor exposure (Rochefort et al., 2002).

Interestingly, a number of studies have reported hippocampus-dependent learning to enhance adult neurogenesis in the hippocampal dentate gyrus and the newborn neurons integrated in the hippocampal network exhibit synaptic plasticity and are also involved in memory formation (Gould et al., 1999a,b; Shors et al., 2001; Shors, 2004; Pham et al., 2005). These reports suggest that the certain types of learning and memory might be formed by the replacement of newborn neurons derived from the

*Corresponding author. Tel: +81-95-819-7033; fax: +81-95-819-7036.
E-mail address: kazuyuki@net.nagasaki-u.ac.jp (K. Shinohara).

Abbreviations: aSVZ, anterior subventricular zone; BrdU, bromodeoxyuridine; CS, conditioned stimulus; PB, phosphate buffer; PBS, phosphate-buffered saline; PBSGT, phosphate-buffered saline containing 1% normal goat serum and 0.3% Triton X-100; PD, postnatal day; RMS, rostral migratory stream; US, unconditioned stimulus.

doi:10.1016/j.neuroscience.2007.07.051

neural stem/progenitor cells in the postnatal brain. From these lines of evidence, it is possible that early olfactory learning involves newborn neurons in the olfactory bulb which originates from neural stem/progenitor cells, which develop in the aSVZ and thereafter migrate via the RMS to the olfactory bulb. To explore this possibility, we therefore investigated whether the olfactory conditioning during the early postnatal period affects the neurogenesis in the olfactory bulb of the rats, using the bromodeoxyuridine (BrdU) –pulse chase method.

EXPERIMENTAL PROCEDURES

Animals

Male and female pups of Long-Evans rats (SLC, Shizuoka, Japan) were used. Dams were housed in polypropylene cages (41× 25×19 cm) with wood shavings, and were kept in an environment with controlled temperature (23 °C) and light (12-h light/dark). Food and water were available *ad libitum*. The litters were culled to 11 on PD 1 (PD 0 is defined as day of birth). All procedures were conducted in accordance with the guidelines of the Institution for Animal Care and the Use Committee of the Nagasaki University. All experiments conformed to international guidelines on the ethical use of animals. All efforts were made to minimize the number of animals used and their suffering.

Olfactory conditioning and sampling schedule

Olfactory conditioning was performed on PD11. During a 30 min training session, the conditioned subjects received continuous exposure of citral odor [conditioned stimulus (CS)] with concurrent electrical foot shock [unconditioned stimulus (US)] (CS/US group). For odor exposure, absorbent cotton (2×2 cm) with 1 μl of citral (Wako, Osaka, Japan) was attached to the ceiling of the training chamber. The foot shock consisted of 15 presentations of a 5-s electrical shock (0.5 mA) which were given at 2 min intervals. For controls, unconditioned subjects received only citral odor (CS/− group). Additional unconditioned subjects that were naïve subjects (−/− group) and shock-only subjects (−/US group), naïve subjects received neither citral odor nor foot-shock and shock-only subjects received only foot shock. The pups were trained in translucent Plexiglas training chamber with a stainless steel grid floor. Immediately after the training, pups were intraperitoneally injected with BrdU (100 mg/kg). Twenty-four hours after the olfactory conditioning, half the pups were deeply anesthetized with diethyl ether and then were perfused intracardially with 25 ml of chilled saline followed by 25 ml of 4% paraformaldehyde in 0.1 M phosphate buffer (PB) and thereafter their brains were quickly removed. The remaining pups were returned to their dams and they were maintained for 2 weeks. Two weeks after such olfactory conditioning, the pups were anesthetized and perfused as described above and their brains were quickly removed. To investigate the survival of newly generated cells during the olfactory conditioning, a group of pups was allowed to survive 8 weeks after the odor conditioning. They were anesthetized with diethyl ether and then were perfused intracardially with 100 ml of chilled saline followed by 100 ml of 4% paraformaldehyde in 0.1 M PB and thereafter their brains were quickly removed.

Immunohistochemistry

The brains were post-fixed in 4% paraformaldehyde in 0.1 M PB overnight at 4 °C, followed by immersion in 20% sucrose in 0.1 M PB for 48 h. The brain sections that were processed for immunohistochemistry were sampled at four distinct antero-posterior levels. The frozen coronal sections with a thickness of 30 μm were made with a cryostat (Leica, Nussloch, Germany) at the olfactory bulb, aSVZ, dentate gyrus and basolateral amygdala levels. The sections were incubated in 2× SSC/formamide at 65 °C for 2 h, and then were treated with 1 N HCl at 37 °C for 20 min, followed by neutralization with 0.15 M sodium borate (pH 8.5) at room temperature for 10 min. After three washes with phosphate-buffered saline (PBS), the sections were incubated with rat anti-BrdU antibody (1:100; Oxford Biotechnology, Oxford, UK) diluted with phosphate-buffered saline containing 1% normal goat serum and 0.3% Triton X-100 (PBSGT) at 4 °C overnight, followed by Alexa-Fluor568-conjugated goat anti-rat IgG (1:200; Molecular Probes, Eugene, OR, USA) and 0.1 μg/ml of Hoechst33258 for a nuclear counterstaining, diluted with PBSGT at room temperature for 2 h. For the double-labeling of the olfactory bulb, the sections were processed for BrdU-immunostaining and then were incubated in primary antibodies at the following dilutions: mouse anti-NeuN antibody 1:500 (Chemicon, Temecula, CA, USA), mouse anti-GFAP antibody 1:150 (Sigma-Aldrich, St. Louis, MO, USA). The sections were incubated with AlexaFluor488-conjugated goat anti-mouse IgG (1:200; Molecular Probes), and 0.1 μg/ml of Hoechst33258 for nuclear counterstaining. After washing with PBS, the sections were mounted, dried and coverslipped with Gel/MountTM, aqueous mounting gel (Biomeda Corporation, Foster City, CA, USA).

Quantification of the number of BrdU-positive cells and the proportion of BrdU-positive cells that co-express neural marker or astroglial marker

Three to five sections in each anatomical region were analyzed. The images were photographed by a digital fluorescent microscope camera (DP70, Olympus, Tokyo, Japan) equipped with a fluorescent microscope (ECLIPSE E600, Nikon, Tokyo, Japan). The number of BrdU-positive cells in the subgranular zone of the dentate gyrus and basolateral amygdala was counted by an observer without any knowledge of the groups. In the olfactory bulb, the number of BrdU-positive cells in the granule cell layer, internal plexiform layer, and mitral cell layer was counted as described above. In the case of aSVZ 24 h after olfactory conditioning, the number of BrdU-positive cells was counted using the Scion image software (Scion Corporation, Frederick, MD, USA) as previously reported (Aida et al., 2002). Double-labeling experiments were analyzed by confocal scanning microscopy (LSM510, Carl Zeiss, Jena, Germany).

Statistical analysis

The data in the present study were statistically analyzed by one-way ANOVA followed by either Fisher's protected LSD post hoc test or unpaired Student's *t*-test.

RESULTS

The effect of olfactory conditioning on the proliferation of the neural stem/progenitor cells

To determine whether the olfactory conditioning affects the proliferation of the neural stem/progenitor cells in the olfactory bulb, we quantified the number of BrdU-positive cells in the olfactory bulb of the conditioned (CS/US group) and unconditioned (CS/− groups) pups 24 h after the olfactory conditioning followed by BrdU injection. Fig. 1A shows the representative immunofluorescence images of BrdU-positive cells in the olfactory bulb of CS/− and CS/US pups. There was no statistical difference in the number of BrdU-positive cells in the olfactory bulb between CS/US and CS/− groups (Fig. 1B). We examined whether olfactory conditioning affects the proliferation of the neural stem/progenitor cells in the aSVZ. We counted the number

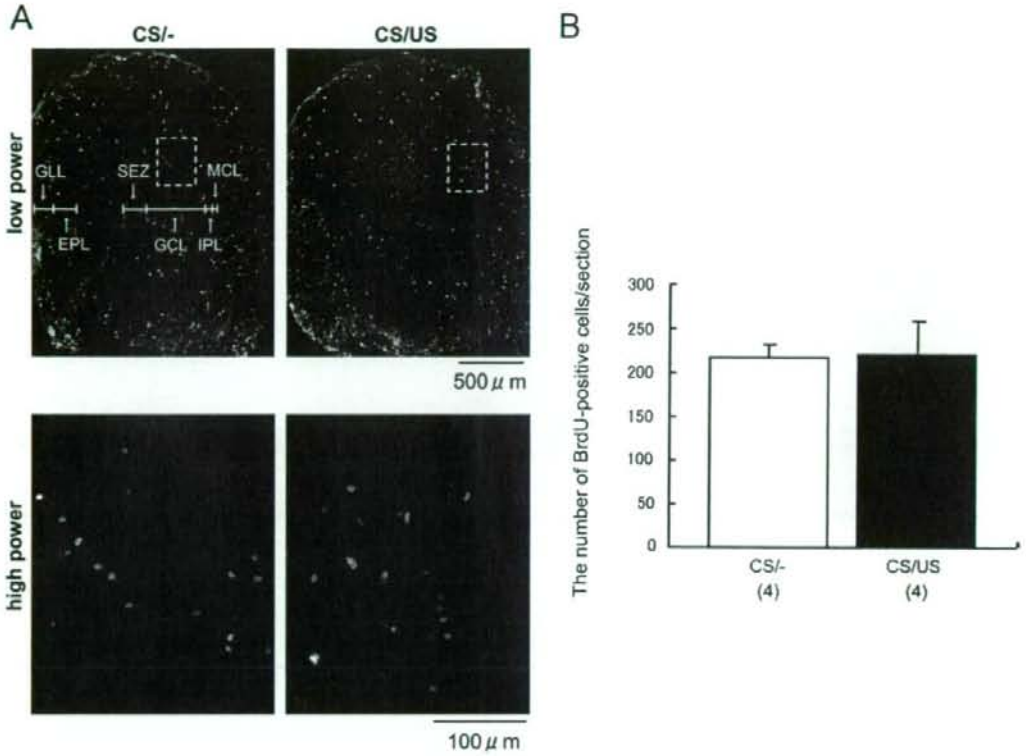

Fig. 1. Olfactory conditioning fails to affect the proliferation of the neural stem/progenitor cells in the olfactory bulb. (A) The representative immunofluorescence images of BrdU-positive cells in the olfactory bulb of CS/− and CS/US pups 24 h after the conditioning. The upper images represent entire olfactory bulb and lower images are the enlargement of the granule cell layer enclosed by dashed rectangle in upper images. SEZ, subependymal zone; GCL, granule cell layer; IPL, interplexi layer; MCL, mitral cell layer; EPL, external plexi layer; GLL, glomerular layer. (B) The number of BrdU-positive cells in the olfactory bulb. The number in parentheses indicates the number of pups.

of BrdU-positive cells in the aSVZ of the conditioned (CS/US group) and unconditioned (CS/−, −/− and −/US groups) pups at 24 h after the olfactory conditioning followed by BrdU injection. Fig. 2A shows the representative immunofluorescence images of BrdU-positive cells in the aSVZ of CS/− and CS/US pups. The number of BrdU-positive cells within the aSVZ in the CS/US group was significantly more abundant in comparison to those in the CS/− control groups (Fig. 2B). In the other groups, no statistical difference was observed in the number of BrdU-positive cells in the aSVZ between the −/− group [758.6± 66.50 (n=4)] and −/US group [816.4±97.31 (n=3)], or between the −/− group [758.6±66.50 (n=4)] and CS/− group [744.7±76.59 (n=7)]. In the subgranular zone of the hippocampal dentate gyrus, there was no statistical difference in the number of BrdU-positive cells between the CS/− group [68.3±3.16 (n=4)] and CS/US group [72.2± 2.45 (n=4)]. Since basolateral amygdala is reported to contain BrdU-positive cells in adult rodents (Wennstrom et al., 2004), we examined the effects of olfactory conditioning on the number of BrdU-positive cells in the basolateral amygdala. However, no significant difference was found in the number of BrdU-positive cells in the basolateral amygdala between the CS/− group [19.4±0.65 (n=4)] and the CS/US group [18.3±1.45 (n=4)].

The effect of olfactory conditioning on the differentiation of neural stem/progenitor cells

We examined whether the olfactory conditioning has any effect on the differentiation of the neural stem/progenitor cells. Therefore, we quantified the number of BrdU-positive cells in the olfactory bulb of conditioned (CS/US group) and unconditioned (CS/−, −/− and −/US groups) pups at 2 weeks after the olfactory conditioning followed BrdU injection, since it takes approximately 2 weeks for neural stem/progenitor cells to migrate and differentiate in the olfactory bulb (Lois and Alvarez-Buylla, 1994). Fig. 3A shows the representative immunofluorescence images of BrdU-positive cells in the olfactory bulb in CS/− and CS/US pups 2 weeks after the conditioning and BrdU injection. The number of BrdU-positive cells in the olfactory

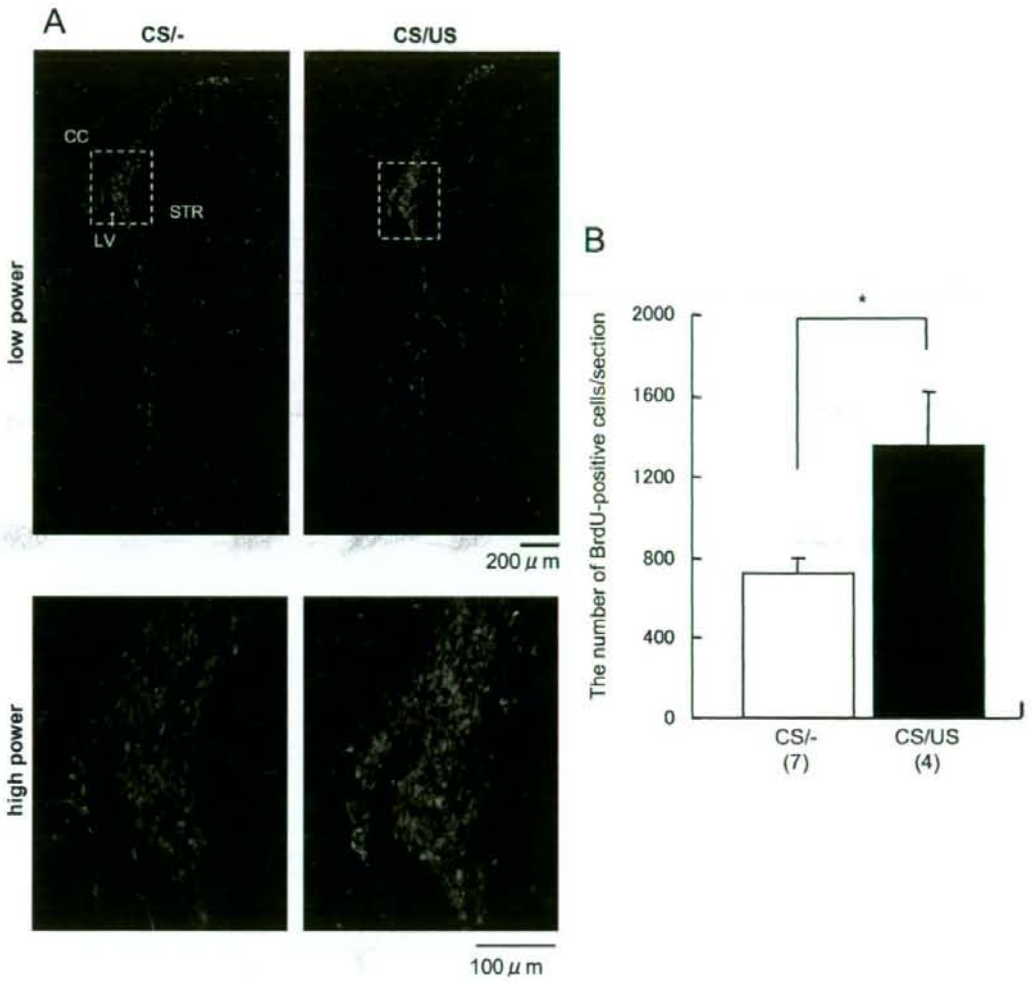

Fig. 2. Olfactory conditioning stimulates the proliferation of the neural stem/progenitor cells in the aSVZ. (A) The representative immunofluorescence images of BrdU-positive cells in the aSVZ of CS/− and CS/US pups 24 h after conditioning. The position of sections that used for cell counting is between Bregma levels +0.3 and +1.2 mm. The upper images represent the entire aSVZ and the lower images show the higher magnification of enclosed area by a dashed rectangle in the upper images. CC, corpus callosum; LV, lateral ventricle; STR, striatum. (B) The number of BrdU-positive cells in the aSVZ. The number in parentheses indicates the number of pups. The asterisk indicates a significant difference ($P<0.01$, one-way ANOVA followed by Fisher's PLSD test).

bulb of CS/US group [578.7±39.62 ($n=14$)] was significantly more abundant in comparison to those in CS/− control groups [477.8±26.12 ($n=18$)] (Fig. 3B). In the other groups, no statistical difference was observed in the number of BrdU-positive cells in the olfactory bulb between the −/− group [485.5±34.54 ($n=9$)] and the −/US group [515.4±8.63 ($n=3$)], or between the −/− group [485.5±34.54 ($n=9$)] and the CS/− group [477.8±26.12 ($n=18$)]. The number of BrdU-positive cells in the olfactory bulb of CS/US group [578.7±39.62 ($n=14$)] tended to increase in comparison to those in −/− control group [485.5±34.54 ($n=9$)] ($P=0.078$), though this difference did not reach a significant level.

We also counted the number of BrdU-positive cells in the aSVZ of conditioned (CS/US group) and unconditioned (CS/− groups) pups 2 weeks after the olfactory conditioning and BrdU injection. There was no statistical difference in the number of BrdU-positive cells between the CS/− group [30.64±6.27 ($n=4$)] and the CS/US group [38.19±8.03 ($n=4$)].

We next examined the effect of olfactory conditioning on the fate of the neural stem/progenitor cells. Therefore, we quantified the proportion of BrdU-positive cells that co-ex-

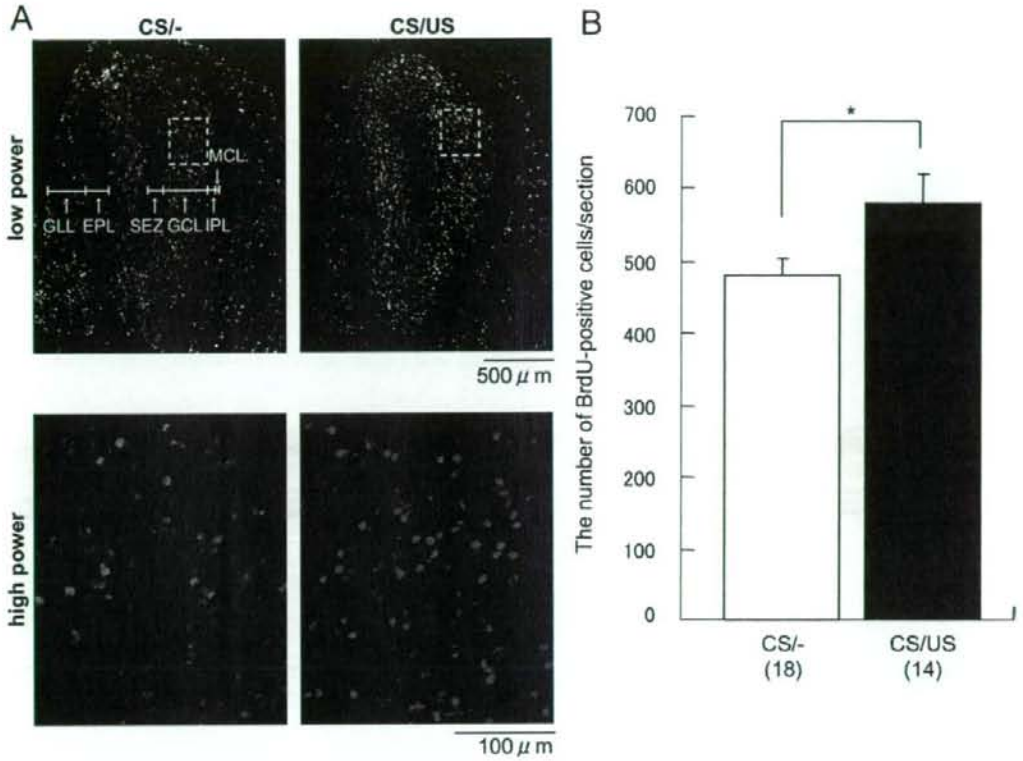

Fig. 3. Olfactory conditioning increases the production of newborn cells in the olfactory bulb. (A) Representative immunofluorescence images of BrdU-positive cells in the olfactory bulb of CS/− and CS/US pups 2 weeks after conditioning. The upper images represent the entire olfactory bulb while the lower images show the enlargement of the granule cell layer enclosed by a dashed rectangle in the upper images. SEZ, subependymal zone; GCL, granule cell layer; IPL, interplexi layer; MCL, mitral cell layer; EPL, external plexi layer; GLL, glomerular layer. (B) The number of BrdU-positive cells in the olfactory bulb. The number in parentheses indicates the number of pups. An asterisk indicates a significant difference ($P<0.05$, one-way ANOVA followed by Fisher's PLSD test).

pressed the neuronal marker NeuN or the astroglial marker GFAP in the granule cell layer of the olfactory bulb in the conditioned (CS/US group) and unconditioned (CS/− group) pups 2 weeks after the olfactory conditioning and BrdU injection. Fig. 4A and 4B exhibit the representative confocal images double-labeled with BrdU-positive cells and NeuN or GFAP in the olfactory bulb. The majority of the BrdU-positive cells co-expressed NeuN, while the BrdU-positive cells with GFAP expression were only sparsely observed. Fig. 4C shows the proportion of the cells double-labeled with either NeuN or GFAP in the olfactory bulb. No difference was observed in the proportion of the BrdU-positive cells co-expressing either NeuN or GFAP between the conditioned (CS/US) group and the unconditioned (CS/−) group.

To investigate the survival of cells newly generated during the olfactory conditioning, we quantified the number of BrdU-positive cells and the proportion of BrdU-positive cells that co-expressed the neuronal marker NeuN or the astroglial marker GFAP in the granule cell layer of the olfactory bulb in the conditioned (CS/US group) and unconditioned (CS/− group) pups 8 weeks after the olfactory conditioning and BrdU injection. Even 8 weeks after the olfactory conditioning followed by BrdU injection, newly generated cells which incorporated BrdU during the olfactory conditioning was observed in the olfactory bulb. There was, however, no statistical difference in the number of BrdU-positive cells between the CS/− [215.4±15.56 (n=4)] and the CS/US group [203.4±6.89 (n=4)]. In regard to the proportion of the BrdU-positive cells co-expressing NeuN, no difference was observed between the CS/− [83.1±1.1% (n=4)] and the CS/US group [84.6±1.2% (n=4)]. Likewise, we could not detect any difference in the proportion of the BrdU-positive cells co-expressing GFAP between the CS/− [14.3±0.6% (n=4)] and the CS/US groups [15.9±1.0% (n=4)].

DISCUSSION

The present study was designed to investigate whether the olfactory conditioning during the early postnatal period

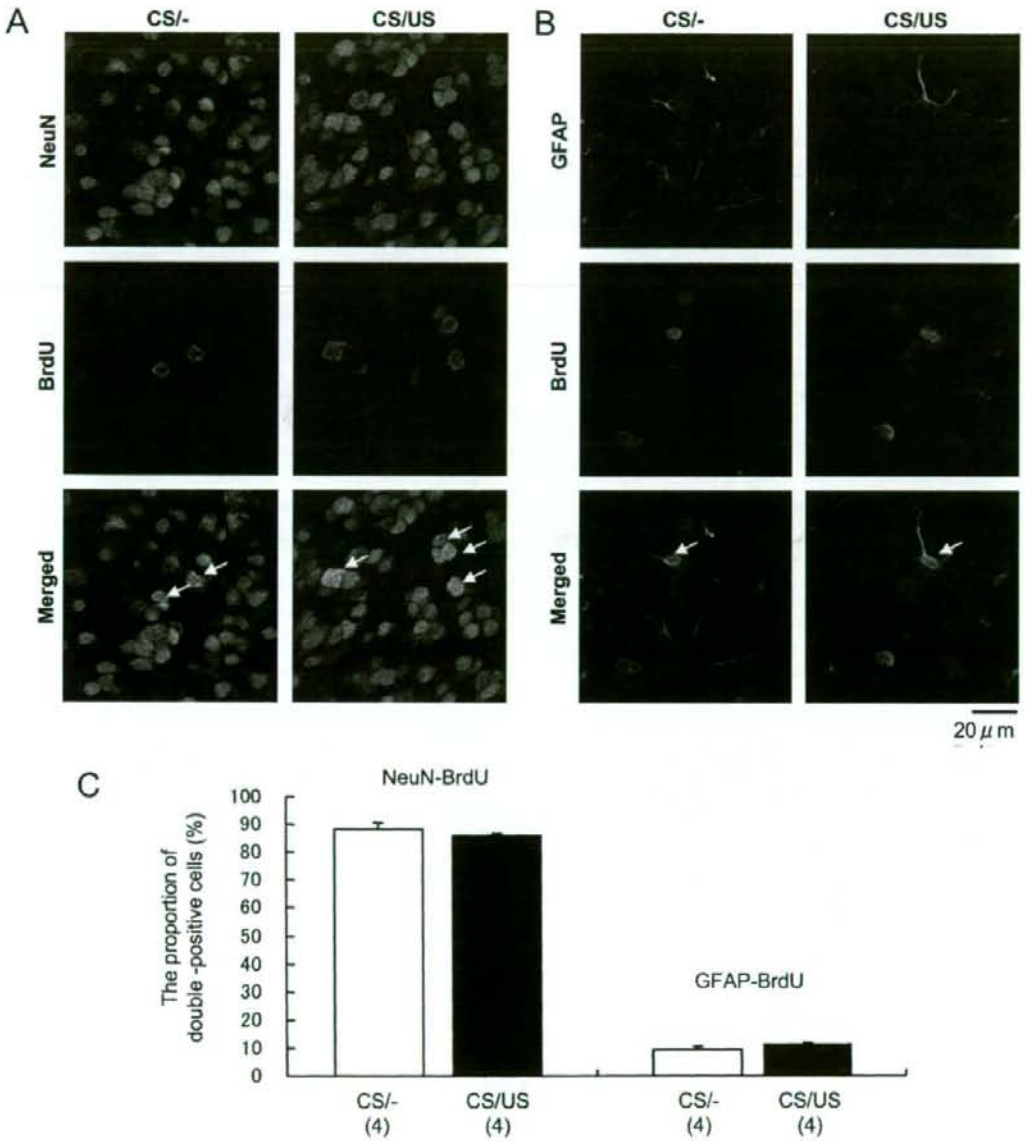

Fig. 4. Most of the newborn cells express the neural marker NeuN. (A) Representative confocal images of the double labeling of BrdU-positive cells with the neural marker NeuN in the olfactory bulb of CS/− and CS/US pups at 2 weeks after conditioning. The arrows in the merged image indicate double-positive cells. (B) The representative confocal images of double labeling of BrdU-positive cells with the astroglial marker GFAP in the olfactory bulb of CS/− and CS/US pups 2 weeks after the conditioning. The arrows in the merged image indicate double-positive cells. (C) The proportion of BrdU–NeuN and BrdU–GFAP double-positive cells in the granule cell layer of the olfactory bulb. The number in parentheses indicates the number of pups.

affects the neurogenesis in the olfactory bulb of rat pups. Using the BrdU–pulse chase method, we found early olfactory conditioning in rats to stimulate the proliferation of the neural stem/progenitor cells in the aSVZ followed by an increase in the number of newborn neurons in the olfactory bulb 2 weeks, but not 8 weeks, later. These results suggest that olfactory conditioning activated the neural stem/progenitor cells in the aSVZ and that the neural stem/progen-

itor cells might migrate rostrally thereby inducing an increase in neurogenesis in the olfactory bulb. To our knowledge, this is the first report to show that olfactory conditioning during the early postnatal period temporally stimulates neurogenesis in the olfactory bulb of rats.

It is well known that the olfactory bulb plays a critical role in odor learning (Wilson and Sullivan, 1994; Sullivan and Wilson, 2003). Since a number of studies have revealed neurogenesis to occur in the postnatal olfactory bulb (Altman, 1969; Luskin, 1993; Lois and Alvarez-Buylla, 1994; Coskun and Luskin, 2002), it is therefore possible that neurogenesis could be involved in the neural plasticity in the olfactory bulb. To explore this possibility, we examined whether the olfactory conditioning in early postnatal rats stimulates the neurogenesis of the neural stem/progenitor cells in the olfactory bulb. As a result, early olfactory conditioning was proven to increase neurogenesis in the olfactory bulb temporally.

We determined where the newborn neurons in the olfactory bulb came from. Since recent studies have revealed that neural stem/progenitor cells exist in the olfactory bulb (Fukushima et al., 2002; Gritti et al., 2002), we examined whether olfactory conditioning in early postnatal rats stimulates the proliferation of neural stem/progenitor cells in the olfactory bulb 24 h after such olfactory conditioning. However, such olfactory conditioning failed to affect the proliferation of neural stem/progenitor cells in the olfactory bulb. Next, we investigated the effect of olfactory conditioning on the proliferation of neural stem/progenitor cells in the aSVZ, in which neural stem/progenitor cells are known to migrate along the RMS and differentiate into interneurons in the olfactory bulb (Altman, 1969; Luskin, 1993; Lois and Alvarez-Buylla, 1994; Kato et al., 2001). As a result, the neural stem/progenitor cells were observed to remarkably proliferate in the aSVZ 24 h after olfactory conditioning, thus suggesting that neurogenesis in the olfactory bulb originated from the neural stem/progenitor cells in the aSVZ.

It is possible that the CS (citral odor) alone or the US (foot shock) alone influenced the proliferation of these neural stem/progenitor cells. However, this possibility is unlikely because we found neither the CS alone nor the US alone to affect the proliferation of neural stem/progenitor cells in the aSVZ.

It has been reported that a considerable number of newborn neural stem/progenitor cells die during migration from SVZ to olfactory bulb (Brunjes and Armstrong, 1996) and a small portion of newborn cells in the SVZ could reach cerebral cortex (Gould et al., 2001; Gould and Gross, 2002). Kato et al. (2001) indicated that two-thirds of newly generated neurons in the granule cell layer of the olfactory bulb were lost during the short survival time (6 weeks). In our present study, it should be noted that the difference in the number of BrdU-positive cells in the aSVZ 24 h after the olfactory conditioning between the CS/− group and CS/US group was more apparatus than that in the olfactory bulb 2 weeks after the olfactory conditioning. Furthermore, we demonstrated that a part of newly generated neurons in the olfactory bulb survived 8 weeks after the olfactory conditioning, but a number of BrdU-positive cells were less than a half of those 2 weeks after the olfactory conditioning and there was no significant difference in the number of BrdU-positive cells between the CS/− group and the CS/US group. Based on both the findings of previous reports and our present results, a part of newly generated cells in the aSVZ during the olfactory conditioning might arrive and survive for a long time in the olfactory bulb, leading the decrease in the difference in the number of BrdU-positive cells 2 and 8 weeks after the conditioning.

Hippocampus-dependent learning, such as water maze learning, trace eyeblink conditioning and contextual fear-conditioning, modulates the neurogenesis in the dentate gyrus, but not in the aSVZ (Gould et al., 1999a; Pham et al., 2005). Shors et al. (2001) demonstrated the neurogenesis in the adult dentate gyrus to be causally involved in the formation of trace eyeblink conditioning using a reagent to diminish the number of adult-generated cells. On the other hand, olfactory conditioning was found to affect the proliferation of neural stem/progenitor cells in the aSVZ, but not in the dentate gyrus in the present study. Thus, the neural stem/progenitor cells in the aSVZ and the dentate gyrus are considered to be independently regulated according to individual learning tasks.

In the present study, we showed early olfactory conditioning to be associated with increases in the proliferation of the neural stem/progenitor cells within the aSVZ followed by increases in neurogenesis in the olfactory bulb at 2 weeks after olfactory conditioning, but its precise mechanism remains unknown. In rats that undergo an olfactory bulbectomy, the neural stem/progenitor cells in the aSVZ continued to proliferate and migrate rostrally (Kirschenbaum et al., 1999). In other studies, olfactory deprivation by naris closure did not affect the proliferation or migration of the majority of neural progenitor cells in the SVZ and RMS (Frazier-Cierpial and Brunjes, 1989; Corotto et al., 1994). Our present study demonstrated that the exposure of the citral odor (CS) alone failed to affect the proliferation of neural progenitor cells in the aSVZ. Based on both the findings of previous reports and our present results, the neural activation in the olfactory bulb by odor stimulation is thus suggested to not be sufficient for the increased neurogenesis caused by olfactory conditioning and olfactory conditioning is suggested to necessarily appear to be associated with odor. Since a number of factors such as growth factors and neuropeptides have been shown to regulate the proliferation of neural stem/progenitor cells in the aSVZ (Gritti et al., 1999; Wagner et al., 1999; Shingo et al., 2003), these factors might associate CS with US in order to regulate the proliferation of neural stem/progenitor cells.

It is known that the neural stem/progenitor cells in the aSVZ migrate long distances and differentiate into interneurons, namely granule cells and periglomerular cells in the olfactory bulb (Altman, 1969; Luskin, 1993; Lois and Alvarez-Buylla, 1994; Zigova et al., 1996). However, it remains to be clarified exactly how newborn neurons are involved in the neural networks of the olfactory bulb. The

granule cells form GABAergic inhibitory synapse to the mitral cells which are the main output neurons from the olfactory bulb. Mutant mice lacking neural cell adhesion molecule have been reported to be deficient in the migration of neural stem/progenitor cells, thus resulting in an impairment of odor discrimination (Gheusi et al., 2000). Similarly, Rochefort et al. (2002) reported an enriched odor environment to increase the number of the newborn granule cells in the olfactory bulb, thereby improving olfactory memory in adult mice. In the present study, we demonstrated the number of newborn neurons in the olfactory bulb to increase by the olfactory conditioning at 2 weeks after, but not 8 weeks after the olfactory conditioning. Further experiments will be required to clarify the role of the temporal stimulation of the neurogenesis by the olfactory conditioning in the brain functions such as olfactory learning and memory.

Acknowledgment—We thank F. Okutani of Kochi Medical School for her helpful discussions and useful advice regarding olfactory conditioning. This work was supported by a Grant-in-aid for Scientific Research (C) (15591231) to K.S. from the Japan Society for the Promotion of Science, and a Grant-in-aid for Young Scientists (B) (17700312) to T.M. from the Japanese Ministry of Education, Culture, Sports, Science and Technology.

REFERENCES

Aida R, Moriya T, Araki M, Akiyama M, Wada K, Wada E, Shibata S (2002) Gastrin-releasing peptide mediates photic entrainable signals to dorsal subsets of suprachiasmatic nucleus via induction of period gene in mice. Mol Pharmacol 61:26–34.

Altman J (1969) Autoradiographic and histological studies of postnatal neurogenesis. IV. Cell proliferation and migration in the anterior forebrain, with special reference to persisting neurogenesis in the olfactory bulb. J Comp Neurol 137:433–457.

Brunjes PC, Armstrong AM (1996) Apoptosis in the rostral migratory stream of the developing rat. Brain Res Dev Brain Res 92:219–222.

Corotto FS, Henegar JR, Maruniak JA (1994) Odor deprivation leads to reduced neurogenesis and reduced neuronal survival in the olfactory bulb of the adult mouse. Neuroscience 61:739–744.

Coskun V, Luskin MB (2002) Intrinsic and extrinsic regulation of the proliferation and differentiation of cells in the rodent rostral migratory stream. J Neurosci Res 69:795–802.

Frazier-Cierpial L, Brunjes PC (1989) Early postnatal cellular proliferation and survival in the olfactory bulb and rostral migratory stream of normal and unilaterally odor-deprived rats. J Comp Neurol 289:481–492.

Fukushima N, Yokouchi K, Kawagishi K, Moriizumi T (2002) Differential neurogenesis and gliogenesis by local and migrating neural stem cells in the olfactory bulb. Neurosci Res 44:467–473.

Gage FH (2002) Neurogenesis in the adult brain. J Neurosci 22: 612–613.

Gheusi G, Cremer H, McLean H, Chazal G, Vincent JD, Lledo PM (2000) Importance of newly generated neurons in the adult olfactory bulb for odor discrimination. Proc Natl Acad Sci U S A 97:1823–1828.

Gould E, Beylin A, Tanapat P, Reeves A, Shors TJ (1999a) Learning enhances adult neurogenesis in the hippocampal formation. Nat Neurosci 2:260–265.

Gould E, Tanapat P, Hastings NB, Shors TJ (1999b) Neurogenesis in adulthood: a possible role in learning. Trends Cogn Sci 3:186–192.

Gould E, Gross CG (2002) Neurogenesis in adult mammals: some progress and problems. J Neurosci 22:619–623.

Gould E, Vail N, Wagers M, Gross CG (2001) Adult-generated hippocampal and neocortical neurons in macaques have a transient existence. Proc Natl Acad Sci U S A 98:10910–10917.

Gritti A, Bonfanti L, Doetsch F, Caille I, Alvarez-Buylla A, Lim DA, Galli R, Verdugo JM, Herrera DG, Vescovi AL (2002) Multipotent neural stem cells reside into the rostral extension and olfactory bulb of adult rodents. J Neurosci 22:437–445.

Gritti A, Frolichsthal-Schoeller P, Galli R, Parati EA, Cova L, Pagano SF, Bjornson CR, Vescovi AL (1999) Epidermal and fibroblast growth factors behave as mitogenic regulators for a single multipotent stem cell-like population from the subventricular region of the adult mouse forebrain. J Neurosci 19:3287–3297.

Kato T, Yokouchi K, Fukushima N, Kawagishi K, Li Z, Moriizumi T (2001) Continual replacement of newly-generated olfactory neurons in adult rats. Neurosci Lett 307:17–20.

Kirschenbaum B, Doetsch F, Lois C, Alvarez-Buylla A (1999) Adult subventricular zone neuronal precursors continue to proliferate and migrate in the absence of the olfactory bulb. J Neurosci 19:2171–2180.

Lois C, Alvarez-Buylla A (1994) Long-distance neuronal migration in the adult mammalian brain. Science 264:1145–1148.

Luskin MB (1993) Restricted proliferation and migration of postnatally generated neurons derived from the forebrain subventricular zone. Neuron 11:173–189.

Okutani F, Yagi F, Kaba H (1999) Gabaergic control of olfactory learning in young rats. Neuroscience 93:1297–1300.

Okutani F, Zhang JJ, Otsuka T, Yagi F, Kaba H (2003) Modulation of olfactory learning in young rats through intrabulbar GABA(B) receptors. Eur J Neurosci 18:2031–2036.

Ono K, Kagawa T, Tsumori T, Yokota S, Yasui Y (2001) Morphological changes and cellular dynamics of oligodendrocyte lineage cells in the developing vertebrate central nervous system. Dev Neurosci 23:346–355.

Pham K, McEwen BS, Ledoux JE, Nader K (2005) Fear learning transiently impairs hippocampal cell proliferation. Neuroscience 130:17–24.

Rochefort C, Gheusi G, Vincent JD, Lledo PM (2002) Enriched odor exposure increases the number of newborn neurons in the adult olfactory bulb and improves odor memory. J Neurosci 22:2679–2689.

Shingo T, Gregg C, Enwere E, Fujikawa H, Hassam R, Geary C, Cross JC, Weiss S (2003) Pregnancy-stimulated neurogenesis in the adult female forebrain mediated by prolactin. Science 299:117–120.

Shors TJ (2004) Memory traces of trace memories: neurogenesis, synaptogenesis and awareness. Trends Neurosci 27:250–256.

Shors TJ, Miesegaes G, Beylin A, Zhao M, Rydel T, Gould E (2001) Neurogenesis in the adult is involved in the formation of trace memories. Nature 410:372–376.

Sullivan RM, Landers M, Yeaman B, Wilson DA (2000) Good memories of bad events in infancy. Nature 407:38–39.

Sullivan RM, Wilson DA (2003) Molecular biology of early olfactory memory. Learn Mem 10:1–4.

Sullivan RM, Wilson DA, Leon M (1989) Norepinephrine and learning-induced plasticity in infant rat olfactory system. J Neurosci 9: 3998–4006.

Sullivan RM, Zyzak DR, Skierkowski P, Wilson DA (1992) The role of olfactory bulb norepinephrine in early olfactory learning. Brain Res Dev Brain Res 70:279–282.

Teicher MH, Blass EM (1976) Suckling in newborn rats: eliminated by nipple lavage, reinstated by pup saliva. Science 193:422–425.

Wagner JP, Black IB, DiCicco-Bloom E (1999) Stimulation of neonatal and adult brain neurogenesis by subcutaneous injection of basic fibroblast growth factor. J Neurosci 19:6006–6016.

Wennstrom M, Hellsten J, Tingstrom A (2004) Electroconvulsive seizures induce proliferation of NG2-expressing glial cells in adult rat amygdala. Biol Psychiatry 55:464–471.